EUROPEAN RESPIRATORY *journal*

FLAGSHIP SCIENTIFIC JOURNAL OF ERS

Early View

Original article

IL-22 and its receptors are increased in human and experimental COPD and contribute to pathogenesis

Malcolm R. Starkey, Maximilian W. Plank, Paolo Casolari, Alberto Papi, Stelios Pavlidis, Yike Guo, Guy J.M. Cameron, Tatt Jhong Haw, Anthony Tam, Ma'en Obiedat, Chantal Donovan, Nicole G. Hansbro, Duc H. Nguyen, Prema Mono Nair, Richard Y. Kim, Jay C. Horvat, Gerard E. Kaiko, Scott K. Durum, Peter A. Wark, Don D. Sin, Gaetano Caramori, Ian M. Adcock, Paul S. Foster, Philip M. Hansbro

Please cite this article as: Starkey MR, Plank MW, Casolari P, *et al*. IL-22 and its receptors are increased in human and experimental COPD and contribute to pathogenesis. *Eur Respir J* 2019; in press (https://doi.org/10.1183/13993003.00174-2018).

IL-22 and its receptors are increased in human and experimental COPD and contribute to pathogenesis

Malcolm R. Starkey[1], Maximilian W. Plank[1], Paolo Casolari[2], Alberto Papi[2], Stelios Pavlidis[3], Yike Guo[3], Guy J.M. Cameron[1], Tatt Jhong Haw[1], Anthony Tam[4,5], Ma'en Obiedat[4,5], Chantal Donovan[1], Nicole G. Hansbro[1,6] Duc H. Nguyen[1], Prema Mono Nair[1], Richard Y. Kim[1], Jay C. Horvat[1], Gerard E. Kaiko[1], Scott K. Durum[7], Peter A. Wark[1], Don D. Sin[4,5], Gaetano Caramori[8], Ian M. Adcock[3], Paul S. Foster[1] and Philip M. Hansbro[1,6]

Affiliations: [1]Priority Research Centres GrowUpWell and Healthy Lungs, School of Biomedical Sciences and Pharmacy, Hunter Medical Research Institute & University of Newcastle, Callaghan, New South Wales, Australia. [2]Interdipartimental Study Center for Inflammatory and Smoke-related Airway Diseases (CEMICEF), Cardiorespiratory and Internal Medicine Section, University of Ferrara, Ferrara, Italy. [3]The Airways Disease Section, National Heart & Lung Institute, Imperial College London, London, UK. [4]The University of British Columbia Center for Heart Lung Innovation, St Paul's Hospital, Vancouver, Canada. [5]Respiratory Division, Department of Medicine, University of British Columbia, Vancouver, BC. [6]Centre for inflammation, Centenary Institute, Sydney, and School of Life Sciences, University of Technology, Ultimo, NSW, Australia. [7]Laboratory of Immunoregulation, Cancer and Inflammation Program, Center for Cancer Research, National Cancer Institute, National Institutes of Health, Frederick, MD, USA. [8]UOC di Pneumologia, Dipartimento di Scienze Biomediche, Odontoiatriche e delle Immagini Morfologiche e Funzionali (BIOMORF), Università di Messina, Italy.

Correspondence: Professor Philip M. Hansbro, Centre for inflammation, Centenary Institute, Sydney, and School of Life Sciences, University of Technology, Ultimo, NSW, Australia. E-mail: p.hansbro@centenary.org.au

Take home message

IL-22 and its receptors are increased in both human and experimental COPD. IL-22 drives neutrophilic inflammation and impaired lung function in experimental chronic obstructive pulmonary disease (195 characters)

This article has supplementary material available from erj.ersjournals.com

Support statement: The National Health and Medical Research Council of Australia, Australian Research Council, The University of Newcastle and Hunter Medical Research Institute

Funding information for this article has been deposited with FundRef.

Conflict of interest: Disclosures can be found alongside the online version of this article at erj.resjournals.com

ABSTRACT Chronic Obstructive Pulmonary Disease (COPD) is the third leading cause of morbidity and death globally. The lack of effective treatments results from an incomplete understanding of the underlying mechanisms driving COPD pathogenesis.

Interleukin (IL)-22 has been implicated in airway inflammation and is increased in COPD patients. However, its roles in the pathogenesis of COPD is poorly understood. Here, we investigated the role of IL-22 in human COPD and in cigarette smoke (CS)-induced experimental COPD.

IL-22 and IL-22 receptor mRNA expression and protein levels were increased in COPD patients compared to healthy smoking or non-smoking controls. IL-22 and IL-22 receptor levels were increased in the lungs of mice with experimental COPD compared to controls and the cellular source of IL-22 included $CD4^+$ T-helper cells, $\gamma\delta$ T-cells, Natural Killer T-cells and group 3 innate lymphoid cells. CS-induced pulmonary neutrophils were reduced in IL-22-deficient (*Il22*$^{-/-}$) mice. CS-induced airway remodelling and emphysema-like alveolar enlargement did not occur in *Il22*$^{-/-}$ mice. *Il22*$^{-/-}$ mice also had improved lung function in terms of airway resistance, total lung capacity, inspiratory capacity, forced vital capacity and compliance.

These data highlight important roles for IL-22 and its receptors in human COPD and CS-induced experimental COPD.

Introduction

Chronic Obstructive Pulmonary Disease (COPD) is the third leading cause of morbidity and death and imposes a significant socioeconomic burden globally [1]. It is a complex, heterogeneous disease characterised by chronic pulmonary inflammation, airway remodelling and emphysema, which are associated with progressive lung function decline [2]. Cigarette smoke (CS) is a major risk factor for COPD [2]. The mainstay therapies for COPD are glucocorticoids, β_2-adrenergic receptor agonists and long-acting muscarinic antagonists [3]. However, these agents only provide symptomatic relief rather than modifying the causal factors or suppressing disease progression [3]. There is emerging interest in altered lung and gut microbiomes and the gut-lung axis that could be modified for therapeutic gain [4, 5]. Nevertheless, there is currently a lack of effective treatments for COPD due to the poor understanding of the underlying mechanisms.

Interleukin (IL)-22 is a member of the IL-10 cytokine family that is implicated in several human diseases, including mucosal-associated infections and inflammatory disorders of the lung [6]. $CD4^+$ T-helper cells, $\gamma\delta$ T-cells, natural killer T (NKT)-cells and group 3 innate lymphoid cells (ILC3) are generally the major cellular sources of IL-22 [6]. Unlike IL-22, expression of the IL-22 receptor (IL-22R) is largely restricted to structural cells. This ligand-receptor distribution permits immune cells to regulate responses of stromal cells and particularly at barrier surfaces such as the lung, where epithelial cells play an active role in initiating, regulating, and resolving immune responses. IL-22R is a cell surface heterodimer consisting of IL-22RA1 and IL-10RB [6]. IL-22RA2 is a naturally occurring IL-22 antagonist that negatively regulates IL-22-induced inflammatory responses [6, 7]. Functional studies in murine systems indicate that IL-22 has immune-regulatory properties in infection,

inflammation, autoimmunity, and cancer [6]. In these models, the functional consequences of IL-22 expression can be either pathologic or protective, depending on the context in which it is expressed. Indeed, increased IL-22 levels and IL-22^{+} cells have been demonstrated in the blood, sputum and lung biopsies of COPD patients [8]. The role of IL-22 in lung antimicrobial defence and the impact of COPD on this defence pathway has been reported [9, 10]. In experimental COPD *Haemophilus influenzae* infection impaired IL-22 production and wild-type and IL-22-deficient ($^{-/-}$) mice had impaired clearance [10]. CS exposure suppressed *Streptococcus pneumoniae* induced IL-22 production and treatment with recombinant IL-22 restored bacterial clearance [11]. Despite this, there is limited knowledge of the role IL-22 plays in COPD pathogenesis independent of respiratory infection.

Here, we investigate its role using gene expression analysis of airway epithelial brushings and parenchymal cores from human COPD patients, an established mouse model of CS-induced experimental COPD that recapitulates the critical features of human disease [4, 12-18], and IL-22 reporter and *Il22*$^{-/-}$ mice [19]. IL-22 and IL-22R mRNA and protein were increased in the airways of mild-moderate COPD patients. IL-22 and IL-22^{+} T-cells and ILC3s were increased in experimental COPD. CS-induced pulmonary neutrophilic inflammation, airway remodelling and emphysema were reduced and lung function was improved in *Il22*$^{-/-}$ mice compared to WT controls, thus implicating IL-22 in COPD pathogenesis.

Methods

Ethics statement, animal details, additional methods and statistical analyses are described in online supplementary material.

Human gene expression. Analysis of IL22, IL22RA1, IL10RB and IL22RA2 in published human array datasets (Accession numbers: GSE5058 and GSE27597) [20-22] was performed using Array Studio software (Omicsoft Corporation, Research Triangle Park, NC, USA).

Mice. Female, 7-8-week-old, WT C57BL/6 mice, *Il17a*$^{eGFP/+}$;*Il22*$^{td\text{-}tomato/+}$ reporter and *Il22*$^{-/-}$ mice on a C57BL/6 background [19].

Experimental COPD. Mice were exposed to normal air or nose-only inhalation of CS for eight weeks in a protocol representative of a pack-a-day smoker as extensively described previously [4, 12-18, 23, 24].

qPCR. Total RNA was extracted from whole lung tissue and blunt-dissected airways and parenchyma and reversed transcribed [13]. mRNA transcripts were determined by real-time quantitative PCR (qPCR, ABIPrism7000, Applied Biosystems, Scoresby, Victoria, Australia) using custom designed primers (Integrated DNA Technologies, Baulkham Hills, New South Wales, Australia) (**supplementary table 1**).

Flow Cytometry. IL-17A$^+$ and IL-22$^+$ CD4$^+$ T-cells, $\gamma\delta$ T-cells, NKT-cells and ILC3s in lung homogenates were determined based on surface marker expression (**supplementary table 2**) [25-27] using a BD FACSAriaIII. Flow cytometry antibodies were from Biolegend (Karrinyup, Australia) or BD Biosciences (North Ryde, Australia) (**supplementary table 3, supplementary figure 1**).

Pulmonary Inflammation. Airway inflammation was assessed by differential enumeration of inflammatory cells in bronchoalveolar lavage fluid (BALF) [12, 14, 28, 29]. BALF supernatants were stored at -20°C for assessment of IL-22 protein levels. Tissue inflammation was assessed by enumeration of inflammatory cells [12-14, 29] and histopathological scoring based on established criteria [30].

ELISA. IL-17A, IL-22, MPO and neutrophil elastase protein levels were quantified with commercially available ELISA kits (R&D Systems or Biolegend) [19].

Immunohistochemistry (IHC). Lungs were perfused, inflated, formalin fixed, paraffin embedded, and sectioned (4μm)[13, 14]. Longitudinal sections of the left lung were deparaffinized and stained with antibodies against IL-22RA1 or IL-22RA2. IHC in human samples is described in online supplement (supplementary tables 4-6)[31]

Airway Remodelling. Airway epithelial (μm^2) and collagen deposition area (μm^2) were assessed in a minimum of four small airways (basement membrane [BM] perimeter <1,000μm) per section [12-14, 17, 18]. Data were quantified using ImageJ software (Version 1.50, NIH) and normalised to BM perimeter (μm).

Alveolar Enlargement. Alveolar diameter was assessed using the mean linear intercept technique [12-14, 17, 18, 32].

Lung Function. Mice were anaesthetised with ketamine (100mg/kg) and xylazine (10mg/kg), tracheas cannulated and attached to Buxco® Forced Manoeuvres

apparatus (DSI, St. Paul, Minnesota, USA) to assess total lung capacity (TLC) [12, 13]. FlexiVent apparatus (FX1 System; SCIREQ, Montreal, Canada) was used to assess lung volume, airway resistance, inspiratory capacity (IC), forced vital capacity (FVC), compliance and elastance (tidal volume: 8mL/kg, respiratory rate: 450 breaths/min) [12, 33, 34].

Results

IL-22 and IL-22R mRNA expression and protein levels are increased in human COPD

We first determined whether the mRNA expression of IL-22, and its receptors IL-22RA1 and IL-10RB and antagonist IL-22RA2 were altered in humans with mild-to-moderate COPD (GOLD Stage I or II Accession: GSE5058 [20, 21, 35]). Pre-existing microarray data from airway epithelial brushings of healthy non-smokers, healthy smokers and COPD patients were interrogated [20]). IL22, IL22RA1, IL10RB and IL22RA2 mRNA expression were not significantly altered in airway epithelial brushings from healthy smokers compared to non-smokers (**Figure 1a-d**). Importantly, however, IL22 (2.01-fold), IL22RA1 (2.48-fold), IL10RB (3.26-fold) and IL22RA2 (1.78-fold) mRNA expression were increased in airway epithelial brushings from patients with mild-to-moderate COPD compared to non-smokers. Similar results were observed when mild-to-moderate COPD was compared to healthy smokers.

We then assessed the mRNA expression of IL-22 and its receptors in pre-existing microarray data from lung parenchyma cores from severe COPD patients (GOLD Stage IV [35] Accession: GSE27597 [22]). There was no change in IL22, IL22RA1, IL10RB or IL22RA2 expression in cores from COPD patients compared to

non-smokers without COPD (**Figure 1e-h**). IL-22, IL-22RA1, IL-22RA2 and IL-10RB were unchanged in peripheral lung tissue from patients with mild emphysema (supplementary figure 2 from GSE8581). There was no significant correlation between pack years and IL-22, IL-22RA1 and IL-22RA2 gene expression in lung tissue (supplementary figure 3 from GSE17770). Using lung cancer as a disease control, no differential expression of IL-22, IL-22RA1, IL-22RA2 or IL-10RB in either bronchial brushings (GSE4115) or lung tissue (GSE1650) between healthy smokers and subjects with lung cancer were observed (**supplementary figures 4-5**).

Finally, we assessed IL-22 and receptor protein levels in human COPD by IHC. The percentage of IL-22^{+} alveolar macrophages and IL-22RA1^{+} and IL-10RB^{+} airway epithelial cells were increased in COPD compared to age- and smoke history-matched smokers with normal lung function (**Figure 2**, **supplementary figure 6** and supplementary tables 6-9). No change in IL-22RA2 was detected (supplementary table 8).

In a separate cohort of COPD patients, IL-22RA1 was also increased in airway epithelial cells of current smokers with COPD compared to non-smokers (**Supplementary Figure 7** and supplementary table 10). When combined with ex-smokers with COPD, these IL-22RA1 signal in the airway epithelium is lost (**Supplementary Figure 7**).

IL-22 and receptor protein levels are increased in the lungs in experimental COPD

We next investigated the expression of IL-22 and its receptors in CS-induced experimental COPD, which models mild-to-moderate COPD. We first confirmed that IL-22 was increased in experimental COPD. *Il22* mRNA was difficult to detect in

mouse lungs, therefore we assessed protein levels by ELISA in both whole lung homogenates (includes both airways and parenchyma) and BALF supernatants. CS-exposure of WT mice resulted in increased IL-22 protein levels in lung homogenates, but not BALF supernatants compared to normal air-exposed controls (**figure 3a-b**). IL-22 protein levels were unaltered following 1 week of CS exposure (**supplementary figure 8**). Collectively, these data show that IL-22 is increased in both human and experimental COPD and are consistent with previous reports [8].

Next, we assessed IL-22 receptor expression in blunt-dissected airways *versus* parenchymal tissue [13]. CS-exposure had no statistically significant effect on *Il22ra1* or *Il10rb* mRNA expression, but did reduce *Il22ra2* expression in the airways compared to normal air-exposed controls (**figure 3c-e**). CS exposure also did not affect *Il22ra1* or *Il22ra2* mRNA expression, but did increase *Il10rb* expression in the parenchyma compared to normal air-exposed controls (**figure 3f-h**). Whilst no statistically significant differences in *Il22ra1* mRNA expression were observed in this model, it is notable that *Il22ra1* mRNA expression was ~10-fold higher in the airways than the parenchyma.

Finally, we assessed IL-22 receptor protein expression in mouse lung tissue sections. CS-exposure resulted in notable increases in both IL-22RA1 and IL-22RA2 protein levels, particularly in airway epithelial cells but also alveolar macrophages (**supplementary figure 9**).

IL-22^{+} CD4^{+} T-cells, γδ T-cells, NKT-cells and ILC3s are increased in the lungs in experimental COPD

Given that IL-22 is increased in both human and experimental COPD, we next defined the cellular source of increased pulmonary IL-22 using *Il17a*$^{eGFP/+}$;*Il22*$^{td-}$

tomato/+ reporter mice that enable the detection of IL-17A$^+$ and IL-22$^+$ cells without *ex vivo* stimulation. CS-exposure of reporter mice resulted in increased numbers of IL-17A$^+$, IL-22$^+$ and IL-17A$^+$IL-22$^+$ CD4$^+$ T-cells, γδ T-cells, NKT-cells and ILC3s compared to normal air-exposed controls (**figure 4a-p**). We then assessed the relative proportions of these cells following CS-exposure (**figure 4q-s**). As previously shown [36], γδT-cells were the dominant source of IL-17A following CS exposure (**figure 4q**). CD4$^+$ T-cells, NKT-cells, and ILC3s were the major IL-22-producing cells (**figure 4r**), whilst NKT-cells were the dominant source of dual IL-17A$^+$IL-22$^+$ cells (**figure 4s**).

CS-induced pulmonary neutrophils were reduced in *Il22*$^{-/-}$ mice

We next investigated whether IL-22 plays a role in the pathogenesis of experimental COPD. WT and *Il22*$^{-/-}$ mice were exposed to normal air or CS for 8 weeks [12-18]. Pulmonary inflammation in BALF was assessed by staining and differential enumeration of inflammatory cells. CS exposure of WT mice resulted in significantly increased total leukocytes, macrophages, neutrophils and lymphocytes compared to normal air-exposed WT controls (**figure 5a-d**). CS-exposed *Il22*$^{-/-}$ mice also had increased numbers of these cells compared to normal air-exposed *Il22*$^{-/-}$ controls. Neutrophils were significantly reduced, but total leukocytes, macrophages and lymphocytes were unaltered in CS-exposed *Il22*$^{-/-}$ mice compared to CS-exposed WT controls.

We then assessed inflammatory cell numbers in lung tissue sections [12-14, 29]. CS exposure of WT mice significantly increased inflammatory cell numbers in the parenchyma compared to normal air-exposed WT controls (**figure 5e-f**). CS-exposed *Il22*$^{-/-}$ mice also had increased parenchymal inflammatory cells compared to

their normal air-exposed controls. Numbers of parenchymal inflammatory cells were not different between CS-exposed *Il22*$^{-/-}$ and WT mice.

Next, histopathology was scored according to a set of custom-designed criteria as described previously [30]. CS exposure of WT mice increased histopathology score, which was characterised by increased airway, vascular and parenchymal inflammation (**figure 5g-k**). CS-exposed *Il22*$^{-/-}$ mice also had increased histopathology, airway, vascular and parenchymal inflammation scores compared to their normal air-exposed controls. *Il22*$^{-/-}$ mice had a small but significant reduction in total histopathology score, compared to CS-exposed WT controls.

We then profiled the mRNA expression of chemokines and cytokines, other than IL-22, that are involved in neutrophil influx into the lung including chemokine (C-X-C motif) ligand (CXCL)1, CXCL2 and IL-17A [37]. CS-exposure of WT mice resulted in significantly increased *Cxcl1*, *Cxcl2* and *Il17a* mRNA expression compared to normal air-exposed WT controls with *Cxcl1* and *Cxcl2* having approximately 200-fold greater expression than *Il17a* (**figure 5l-n**). CS-exposed *Il22*$^{-/-}$ mice also had increased expression of *Cxcl1* and *Il17a*, but not *Cxcl2* compared to normal air-exposed *Il22*$^{-/-}$ controls. There was a significant reduction in *Cxcl2*, but not *Cxcl1* or *Il17a* mRNA expression in CS-exposed *Il22*$^{-/-}$ mice compared to CS-exposed WT controls. Protein levels of IL-17A, MPO and neutrophil elastase were increased in CS-exposed WT mice, but were unaltered in *Il22*$^{-/-}$ mice (**supplementary figure 10**).

CS-induced increases in airway epithelial area, collagen deposition and emphysema-like alveolar enlargement do not occur in *Il22*$^{-/-}$ mice

We have previously shown that CS-exposed WT mice develop small airway remodelling (increased epithelial area), fibrosis (collagen deposition) and emphysema-like alveolar enlargement after 8 weeks of CS exposure [12-14, 17, 18, 32]. Thus, we next determined whether IL-22 contributes to these disease features. In agreement with our previous studies, CS exposure of WT mice increased small airway epithelial cell area compared to normal air-exposed WT controls (**figure 6a-b**). In contrast, CS-exposed *Il22*$^{-/-}$ mice had no change in airway epithelial cell area compared to normal air-exposed *Il22*$^{-/-}$ controls.

CS-exposed WT mice had increased collagen deposition compared to normal air-exposed WT controls (**figure 6c-d**). However, CS-exposed *Il22*$^{-/-}$ mice did not have increased collagen deposition compared to *Il22*$^{-/-}$ normal air-exposed controls.

CS-exposed WT mice had significantly increased alveolar diameter compared to normal air-exposed WT controls (**figure 6e-f**). CS-exposed *Il22*$^{-/-}$ mice did not have increased alveolar diameter compared normal air-exposed *Il22*$^{-/-}$ controls.

As a result of the relatively small differences in airway epithelial area, collagen deposition and alveolar diameter the differences were not statistically different between CS-exposed *Il22*$^{-/-}$ mice and CS-exposed WT controls.

CS-induced lung function impairment is improved in *Il22*$^{-/-}$ mice

We next assessed the role of IL-22 in CS-induced impairment of lung function, measured in terms of lung volume, airway resistance, TLC, IC, FVC and compliance. CS-exposed WT mice had increases in all of these parameters compared to normal air-exposed WT controls (**Figure 7a-f**). In CS-exposed *Il22*$^{-/-}$ mice none of these lung function parameters were significantly different compared to normal air-exposed *Il22*$^{-/-}$ controls. Again, likely due to small changes in mild-moderate experimental COPD,

these lung function parameters were not significantly altered in CS-exposed *Il22*$^{-/-}$ mice compared to CS-exposed WT controls. However, CS-exposed *Il22*$^{-/-}$ mice had similar lung function to air-exposed WT controls.

We also assessed tissue elastance and found a non-significant reduction in CS-exposed WT mice that was not different in *Il22*$^{-/-}$ mice (**supplementary figure 11**).

Discussion

Here, we demonstrate that IL-22 plays a previously undefined role in the pathogenesis of CS-induced experimental COPD. IL-22 and its receptors were increased in both human and experimental COPD. We show for the first-time using IL-22 reporter mice, that elevated lung IL-22 levels in experimental COPD result from increased IL-22^{+} CD4^{+} T-cells, $\gamma\delta$ T-cells, NKT-cells and ILC3s. We also demonstrated that CS-induced neutrophilic airway inflammation, was reduced in *Il22*$^{-/-}$ mice compared to WT controls. Furthermore, *Il22*$^{-/-}$ mice did not develop CS-induced airway remodelling and emphysema and had improved lung function that was comparable to normal air-exposed controls. Hence, this study provides new insights into the roles of IL-22 in the pathogenesis of COPD.

The presence or absence of IL-22 may affect resident microbiota. Indeed, we have reviewed the pathogenic roles for gut and lung microbiota in the development of COPD [5, 38, 39]. To minimise the influence of altered microbiota WT and *Il22*$^{-/-}$ mice were derived from the same breeding pairs, maintained in the same facility and used experimentally at the same time, and so they would be expected to have very similar microbiomes.

Using pre-existing microarray datasets, we show that IL-22 and IL-22R mRNA expression were increased in airway epithelial cells from patients with mild-to-

moderate COPD [20]. However, IL-22 and IL-22R mRNA were unaltered in lung parenchymal cores in severe COPD [22]. Our data are supported by studies that show increased IL-22 protein levels and IL-22$^+$ immune cells in blood, sputum and lung biopsies of COPD patients (reviewed in [8]). However, there are limited reports of IL-22 receptor expression in COPD. Neutrophil proteases have been shown alter IL-22R-dependent antimicrobial defence in COPD but there was no change in IL22RA1 mRNA expression in lung tissue or primary cultures of proximal airway epithelial cells from COPD patients compared to healthy controls [9]. IL-10RB and IL-22RA2 have not been assessed in COPD. Consistent with our human data, IL-22 was also increased in lung tissue homogenates in experimental COPD after 8 weeks but not before the development of disease upon 1 week of CS exposure. IL-22 receptor mRNA expression was different between human and mouse. However, at the protein level, IL-22RA1 and RA2 were visually increased in the airway epithelium of CS-exposed mice, which was consistent with changes at the mRNA level in humans. IL-22 receptors were also increased at protein level in human COPD. Collectively, our data show that IL-22 and its receptors are increased in both human and experimental COPD. However, the expression of IL-22 and its receptors is heterogenous and is influenced by tissue location and disease severity.

Given that IL-22 was increased in the lungs in experimental COPD, we utilised IL-17A and IL-22 dual reporter mice that facilitate the identification of IL-17A- and IL-22-expressing immune cells without *ex vivo* stimulation or cell fixation. This enables a more accurate determination of the *in vivo* lung environment. We show for the first time that CS exposure induced IL-22 production from CD4$^+$ T-cells, $\gamma\delta$ T-cells, NKT-cells and ILC3s, which are the major cellular sources of IL-22 and all these cell subsets have known roles in COPD pathogenesis [36, 40, 41]. However,

the individual contribution of each of these cells to IL-22 production and COPD pathogenesis, especially in humans remains to be fully elucidated.

Previously, the role of IL-22 in the pathogenesis of COPD was largely unknown. We addressed this gap in knowledge using an established mouse model of tightly controlled chronic nose-only CS-induced experimental COPD [12-18]. Our models are representative of a pack-a-day smoker [24]. We have consistently shown that 8 weeks of CS exposure in our models is sufficient to induce the hallmark features of human COPD: chronic inflammation, airway remodelling, emphysema and impaired lung function [12-18]. This 8-week time point was specifically chosen to investigate the underlying pathogenic mechanism(s) during the early stages (GOLD I/II) and identify potential therapeutic targets to halt the progression of COPD.

Using this established model, we show for the first time that IL-22 contributes to COPD pathogenesis independently of infectious exacerbations. *Il22*$^{-/-}$ mice had reduced airway neutrophils, which was associated with decreased in *Cxcl2* mRNA expression. CXCL1 and CXCL2 are the mouse orthologues/homologues of human IL-8 and have critical roles in neutrophil influx into the airways following CS-exposure [42]. It has been suggested that improper activation of neutrophils lies at the core of COPD pathology, and mechanisms regulating their function are potential therapeutic targets [43]. However, *Il22*$^{-/-}$ mice were protected from the increases in MPO or neutrophil elastase levels. *Il22*$^{-/-}$ mice also had decreased lung tissue inflammation indicated by reduced histopathological score. This is consistent with a previous report showing that administration of recombinant IL-22 (rIL-22) into the lung increased tissue inflammation [44].

We also demonstrate, as we have shown previously, that increases in airway epithelial area, collagen deposition around small airways and emphysema-like

alveolar enlargement occur following chronic CS-exposure in WT mice [12-18]. Notably, these features did not develop in *Il22*$^{-/-}$ mice compared to normal air-exposed *Il22*$^{-/-}$ controls, although the changes were not significant between CS-exposed *Il22*$^{-/-}$ mice and CS-exposed WT controls. IL-22 is essential for lung epithelial cell repair following influenza virus infection and is implicated in renal fibrosis [45, 46]. Others have shown that mice lacking IL-22 have delayed bacterial clearance and increased alveolar wall thickening and airway remodelling [10]. Administration of rIL-22 with or without acute CS-exposure induced airway epithelial thickening and collagen deposition, although this was not quantified [44].

Our study is the first report on the role of IL-22 in regulating multiple lung function parameters, particularly in models of COPD. We show that *Il22*$^{-/-}$ mice have improved lung function in terms of lung volumes, airway resistance, TLC, IC, FVC and compliance that are comparable to normal air-exposed WT mice. One previous report in an acute CS-exposure model showed increased airway resistance following administration of rIL-22 [44], however ours is the first study to assess lung function in *Il22*$^{-/-}$ mice.

The absence of IL-22 in CS-exposed *Il22*$^{-/-}$ mice suppressed both airway remodelling and concomitantly the impairment of lung function in experimental COPD. Indeed CS-exposed *Il22*$^{-/-}$ mice were protected against increases in epithelial area, collagen deposition and emphysema compared to normal air-exposed controls. Airway remodelling involving epithelial hyperplasia and fibrosis are important in driving resistance to airflow [17, 18]. Emphysema leads to apparent increases in total lung and inspiratory capacity and tissue compliance, which results from the loss of alveolar and parenchymal tissue. In line with the protection against airway remodelling and emphysema-like alveolar enlargement, CS-exposed *Il22*$^{-/-}$ mice

were also protected from impaired lung function and changes in airway resistance, total lung and inspiratory capacity and tissue compliance.

In summary, our study demonstrates previously unrecognised roles for IL-22 in COPD pathogenesis. It highlights the potential role of IL-22 in chronic lung diseases, which may be a useful biomarker in the diagnosis and/or prognosis of COPD patients. Furthermore, using a clinically-relevant and established model of experimental COPD, our study demonstrates that IL-22 promotes CS-induced pulmonary neutrophilic inflammation, airway remodelling and lung function impairment. However, inhibiting IL-22 may increase the risk of exacerbations due to its central role in pathogen clearance. Therefore, caution in therapeutic approaches targeting IL-22 signalling are required. The relationships between IL-22 and genetic factors, infections/colonisation and phenotypes in COPD remain to be defined.

Acknowledgements

This study was supported by grants from the National Health and Medical Research Council (NHMRC) of Australia and the Australian Research Council (ARC). M.R.S was supported by an NHMRC Early Career Research Fellowship and is supported by an Australian Research Council (ARC) Discovery Early Career Researcher Award (DECRA) fellowship. C.D. is supported by an NHMRC Early Career Research. Fellowship I.M.A is supported by Wellcome Trust grant. P.M.H is supported by an NHMRC Principal Research Fellowship (1079187) and by a Brawn Fellowship, Faculty of Health & Medicine, the University of Newcastle. We acknowledge Prof. Dale Godfrey, The University of Melbourne for αGalCer tetramers, Kristy Wheeldon and Nathalie Kiaos for CS exposure of mice, Tegan Moore for assistance with data

generation and Jessica Weaver for assistance with *Il22*$^{-/-}$ and reporter mouse colonies.

Conflict of interest

PMH reports funding/consultancies from Pharmaxis, AstraZeneca, Sanofi, Pharmakea, Ausbio, and Allakos outside the submitted work. Other authors declared no conflict of interest, financial or otherwise.

Figure 1: IL-22 and IL-22R mRNA expression are increased in airway epithelial brushings from mild-moderate human COPD patients compared to healthy smokers and non-smokers. Microarray data from airway epithelial cells from healthy human non-smokers (NS), healthy smokers without COPD (Smoker) and COPD patients with Global Initiative for Chronic Obstructive Lung Disease (GOLD) stage I (Mild) or II (Moderate) disease (Accession: GSE5058 [20]) were interrogated. **(a)** IL22 **(b)** IL22RA1, **(c)** IL10RB, **(d)** IL22RA2 mRNA expression. Microarray data from lung parenchymal cores from human healthy non-smokers (NS) and COPD patients with GOLD) stage IV (severe) disease (Accession: GSE27597 [22]) were interrogated. **(e)** IL22 **(f)** IL22RA1, **(g)** IL10RB, **(h)** IL22RA2 mRNA expression. Data are expressed as $\log_2$ intensity robust multi-array average signals. The Benjamini–Hochberg method for adjusted P value/false discovery rate (FDR) was used to analyse differences between NS, Smokers and COPD patients. * = $p<0.005$ compared to COPD. ns = not significant.

Figure 2: IL-22, IL-22RA1 and IL-10Rb, but not IL-22RA2 protein is increased in human COPD. IHC for IL-22 and its receptors in peripheral lung from smokers with mild-to-moderate stable COPD and compared to age- and smoke history-matched smokers with normal lung function. (**a**) IL-22^{+} alveolar macrophages, (**b**) IL-22RA1^{+} alveolar macrophages, (**c**) IL-22RA1^{+} airway epithelial cells, (**d**) IL-10RB^{+} alveolar macrophages, (**e**) IL-10RB^{+} airway epithelial cells. Data are presented as mean ± SEM, n = 12.

Figure 3: IL-22 protein levels are increased in the lungs of CS-exposed mice with experimental COPD. Wild-type (WT) C57BL/6 mice were exposed to normal air or CS for 8 weeks. IL-22 protein levels in (**a**) lung homogenates and (**b**) bronchoalveolar lavage fluid (BALF) supernatants were assessed by ELISA. In separate experiments, airways and parenchyma were blunt-dissected and IL-22 receptor mRNA expression assessed. Airway (**c**) *Il22ra1,* (**d**) *Il10rb*, (**e**) *Il22ra2* and parenchymal (**f**) *Il22ra1,* (**g**) *Il10rb* and (**h**) *Il22ra2* mRNA expression. Data are presented as mean ± SEM, n = 6, with another independent experiment showing similar results. Two-tailed Mann-Whitney t-test was used to analyse differences between two groups, whereby * = $p<0.05$ compared to normal air-exposed WT controls.

Figure 4: IL-22^{+} CD4^{+} T-cells, γδ T-cells, NKT-cells and ILC3s are increased in the lungs of CS-exposed mice with experimental COPD. *Il17a*$^{eGFP/+}$*;Il22*$^{td\text{-}tomato/+}$ reporter mice were exposed to normal air or CS for 8 weeks and the cellular source of IL-17A and IL-22 in the lung was assessed by flow cytometry. (**a**) Representative FACS plot of IL-17A^{+} and IL-22^{+} CD4^{+} T-cells. Total numbers of (**b**) IL-17A^{+}, (**c**) IL-

22^+ and (**d**) IL-$17A^+$IL-22^+ $CD4^+$ T-cells in the lung. (**e**) Representative FACS plot of IL-$17A^+$ and IL-22^+ γδ T-cells. Total numbers of (**f**) IL-$17A^+$, (**g**) IL-22^+ and (**h**) IL-$17A^+$IL-22^+ γδ T-cells in the lung. (**i**) Representative FACS plot of IL-$17A^+$ and IL-22^+ NKT-cells. Total numbers of (**j**) IL-$17A^+$, (**k**) IL-22^+ and (**l**) IL-$17A^+$IL-22^+ NKT-cells in the lung. (**m**) Representative FACS plot of IL-$17A^+$ and IL-22^+ ILC3s. Total numbers of (**n**) IL-$17A^+$, (**o**) IL-22^+ and (**p**) IL-$17A^+$IL-22^+ ILC3 cells in the lung. Relative proportion of $CD4^+$ T-cells, γδ T-cells, NKT-cells and ILC3s expressing (**q**) IL-17A, (**r**) IL-22 and (**s**) IL-17 and IL-22. Data are presented as mean ± SEM, n = 6, with another independent experiment showing similar results. Two-tailed Mann-Whitney t-test was used to analyse differences between two groups, whereby * = $p<0.05$ compared to normal air-exposed controls.

Figure 5: CS-induced pulmonary inflammation is reduced in *Il22*$^{-/-}$ mice. Wild-type (WT) and IL-22-deficient (*Il22*$^{-/-}$) C57BL/6 mice were exposed to normal air or CS for 8 weeks to induce experimental COPD. (**a**) Total leukocytes, (**b**) macrophages, (**c**) neutrophils and (**d**) lymphocytes in bronchoalveolar lavage fluid (BALF). (**e**) Representative images of parenchymal inflammatory cells. (**f**) Numbers of parenchymal inflammatory cells per high powered field. (**g**) Representative images of lung histopathology scoring. (**h**) Total histopathology score in lung sections and scores specifically in the (**i**) airway, (**j**) vascular and (**k**) parenchymal regions. (**l**) *Cxcl1*, (**m**) *Cxcl2* and (**n**) *Il17a* mRNA expression in lung homogenates. Data are presented as mean ± SEM, n = 6, with another independent experiment showing similar results.. The one-way analysis of variance with Bonferroni post-test analysed differences between 3 or more groups, whereby * = $p<0.05$ compared to normal air-exposed controls.

Figure 6: CS-induced increases in airway epithelial area, collagen deposition and emphysema-like alveolar enlargement do not occur in *Il22*$^{-/-}$ mice. Wild-type (WT) and IL-22-deficient (*Il22*$^{-/-}$) C57BL/6 mice were exposed to normal air or CS for 8 weeks to induce experimental COPD. (**a**) Representative images of small airway epithelium. (**b**) Small airway epithelial thickness in terms of epithelial cell area (μm^2) per basement membrane (BM) perimeter (μm). (**c**) Representative images of collagen deposition around small airways. (**d**) Area of collagen deposition (μm^2) per BM perimeter (μm). (**e**) Representative images of alveolar structure. (**f**) Alveolar diameter (μm). Data are presented as mean ± SEM, n = 6, with another independent experiment showing similar results. The one-way analysis of variance with Bonferroni post-test analysed differences between 3 or more groups, whereby * = $p<0.05$ compared to normal air-exposed controls.

Figure 7: CS-induced lung function impairment is improved in *Il22*$^{-/-}$ mice. Wild-type (WT) and IL-22-deficient (*Il22*$^{-/-}$) C57BL/6 mice were exposed to normal air or CS for 8 weeks to induce experimental COPD. Lung function was assessed in terms of (**a**) lung volume from pressure volume loops, (**b**) airway resistance, (**c**) total lung capacity, (**d**) inspiratory capacity, (**e**) forced vital capacity and (**f**) compliance. Data are presented as mean ± SEM, n = 6, with another independent experiment showing similar results. The one-way analysis of variance with Bonferroni post-test analysed differences between 3 or more groups, whereby * = $p<0.05$ compared to normal air-exposed controls.

References

1. Lozano R, Naghavi M, Foreman K, Lim S, Shibuya K, Aboyans V, Abraham J, Adair T, Aggarwal R, Ahn SY, Alvarado M, Anderson HR, Anderson LM, Andrews KG, Atkinson C, Baddour LM, Barker-Collo S, Bartels DH, Bell ML, Benjamin EJ, Bennett D, Bhalla K, Bikbov B, Bin Abdulhak A, Birbeck G, Blyth F, Bolliger I, Boufous S, Bucello C, Burch M, Burney P, Carapetis J, Chen H, Chou D, Chugh SS, Coffeng LE, Colan SD, Colquhoun S, Colson KE, Condon J, Connor MD, Cooper LT, Corriere M, Cortinovis M, de Vaccaro KC, Couser W, Cowie BC, Criqui MH, Cross M, Dabhadkar KC, Dahodwala N, De Leo D, Degenhardt L, Delossantos A, Denenberg J, Des Jarlais DC, Dharmaratne SD, Dorsey ER, Driscoll T, Duber H, Ebel B, Erwin PJ, Espindola P, Ezzati M, Feigin V, Flaxman AD, Forouzanfar MH, Fowkes FG, Franklin R, Fransen M, Freeman MK, Gabriel SE, Gakidou E, Gaspari F, Gillum RF, Gonzalez-Medina D, Halasa YA, Haring D, Harrison JE, Havmoeller R, Hay RJ, Hoen B, Hotez PJ, Hoy D, Jacobsen KH, James SL, Jasrasaria R, Jayaraman S, Johns N, Karthikeyan G, Kassebaum N, Keren A, Khoo JP, Knowlton LM, Kobusingye O, Koranteng A, Krishnamurthi R, Lipnick M, Lipshultz SE, Ohno SL, Mabweijano J, MacIntyre MF, Mallinger L, March L, Marks GB, Marks R, Matsumori A, Matzopoulos R, Mayosi BM, McAnulty JH, McDermott MM, McGrath J, Mensah GA, Merriman TR, Michaud C, Miller M, Miller TR, Mock C, Mocumbi AO, Mokdad AA, Moran A, Mulholland K, Nair MN, Naldi L, Narayan KM, Nasseri K, Norman P, O'Donnell M, Omer SB, Ortblad K, Osborne R, Ozgediz D, Pahari B, Pandian JD, Rivero AP, Padilla RP, Perez-Ruiz F, Perico N, Phillips D, Pierce K, Pope CA, 3rd, Porrini E, Pourmalek F, Raju M, Ranganathan D, Rehm JT, Rein DB, Remuzzi G, Rivara FP, Roberts T, De Leon FR, Rosenfeld LC, Rushton L, Sacco RL, Salomon JA, Sampson U, Sanman E, Schwebel DC, Segui-Gomez M, Shepard DS, Singh D, Singleton J, Sliwa K, Smith E, Steer A, Taylor JA, Thomas B, Tleyjeh IM, Towbin JA, Truelsen T, Undurraga EA, Venketasubramanian N, Vijayakumar L, Vos T, Wagner GR, Wang M, Wang W, Watt K, Weinstock MA, Weintraub R, Wilkinson JD, Woolf AD, Wulf S, Yeh PH, Yip P, Zabetian A, Zheng ZJ, Lopez AD, Murray CJ, AlMazroa MA, Memish ZA. Global and regional mortality from 235 causes of death for 20 age groups in 1990 and 2010: a systematic analysis for the Global Burden of Disease Study 2010. *Lancet (London, England)* 2012: 380(9859): 2095-2128.
2. Keely S, Talley NJ, Hansbro PM. Pulmonary-intestinal cross-talk in mucosal inflammatory disease. *Mucosal immunology* 2012: 5(1): 7-18.
3. Barnes PJ. Corticosteroid resistance in patients with asthma and chronic obstructive pulmonary disease. *The Journal of allergy and clinical immunology* 2013: 131(3): 636-645.
4. Fricker M GB, Mateer S, Jones B, Kim RY, Gellatly SL, Jarnicki AG, Powell N, Oliver BG, Radford-Smith G, Talley NJ, Walker MM, Keely S, Hansbro PM. . Chronic smoke exposure induces systemic hypoxia that drives intestinal dysfunction. . *JCI insight* 2018(In Press).
5. Budden KF, Gellatly SL, Wood DL, Cooper MA, Morrison M, Hugenholtz P, Hansbro PM. Emerging pathogenic links between microbiota and the gut-lung axis. *Nature reviews Microbiology* 2017: 15(1): 55-63.
6. Dudakov JA, Hanash AM, van den Brink MR. Interleukin-22: immunobiology and pathology. *Annual review of immunology* 2015: 33: 747-785.

7. Xu W, Presnell SR, Parrish-Novak J, Kindsvogel W, Jaspers S, Chen Z, Dillon SR, Gao Z, Gilbert T, Madden K, Schlutsmeyer S, Yao L, Whitmore TE, Chandrasekher Y, Grant FJ, Maurer M, Jelinek L, Storey H, Brender T, Hammond A, Topouzis S, Clegg CH, Foster DC. A soluble class II cytokine receptor, IL-22RA2, is a naturally occurring IL-22 antagonist. *Proceedings of the National Academy of Sciences of the United States of America* 2001: 98(17): 9511-9516.
8. Le Rouzic O, Pichavant M, Frealle E, Guillon A, Si-Tahar M, Gosset P. Th17 cytokines: novel potential therapeutic targets for COPD pathogenesis and exacerbations. *The European respiratory journal* 2017: 50(4).
9. Guillon A, Jouan Y, Brea D, Gueugnon F, Dalloneau E, Baranek T, Henry C, Morello E, Renauld JC, Pichavant M, Gosset P, Courty Y, Diot P, Si-Tahar M. Neutrophil proteases alter the interleukin-22-receptor-dependent lung antimicrobial defence. *The European respiratory journal* 2015: 46(3): 771-782.
10. Sharan R, Perez-Cruz M, Kervoaze G, Gosset P, Weynants V, Godfroid F, Hermand P, Trottein F, Pichavant M, Gosset P. Interleukin-22 protects against non-typeable Haemophilus influenzae infection: alteration during chronic obstructive pulmonary disease. *Mucosal immunology* 2017: 10(1): 139-149.
11. Pichavant M, Sharan R, Le Rouzic O, Olivier C, Hennegrave F, Remy G, Perez-Cruz M, Kone B, Gosset P, Just N, Gosset P. IL-22 Defect During Streptococcus pneumoniae Infection Triggers Exacerbation of Chronic Obstructive Pulmonary Disease. *EBioMedicine* 2015: 2(11): 1686-1696.
12. Beckett EL, Stevens RL, Jarnicki AG, Kim RY, Hanish I, Hansbro NG, Deane A, Keely S, Horvat JC, Yang M, Oliver BG, van Rooijen N, Inman MD, Adachi R, Soberman RJ, Hamadi S, Wark PA, Foster PS, Hansbro PM. A new short-term mouse model of chronic obstructive pulmonary disease identifies a role for mast cell tryptase in pathogenesis. *The Journal of allergy and clinical immunology* 2013: 131(3): 752-762.
13. Haw TJ, Starkey MR, Pavlidis S, Fricker M, Arthurs AL, Mono Nair P, Liu G, Hanish I, Kim RY, Foster PS, Horvat JC, Adcock IM, Hansbro PM. Toll-like receptor 2 and 4 have Opposing Roles in the Pathogenesis of Cigarette Smoke-induced Chronic Obstructive Pulmonary Disease. *American journal of physiology Lung cellular and molecular physiology* 2017: ajplung.00154.02017.
14. Haw TJ, Starkey MR, Nair PM, Pavlidis S, Liu G, Nguyen DH, Hsu AC, Hanish I, Kim RY, Collison AM, Inman MD, Wark PA, Foster PS, Knight DA, Mattes J, Yagita H, Adcock IM, Horvat JC, Hansbro PM. A pathogenic role for tumor necrosis factor-related apoptosis-inducing ligand in chronic obstructive pulmonary disease. *Mucosal immunology* 2016: 9(4): 859-872.
15. Hsu AC, Starkey MR, Hanish I, Parsons K, Haw TJ, Howland LJ, Barr I, Mahony JB, Foster PS, Knight DA, Wark PA, Hansbro PM. Targeting PI3K-p110alpha Suppresses Influenza Virus Infection in Chronic Obstructive Pulmonary Disease. *American journal of respiratory and critical care medicine* 2015: 191(9): 1012-1023.
16. Hsu AC, Dua K, Starkey MR, Haw TJ, Nair PM, Nichol K, Zammit N, Grey ST, Baines KJ, Foster PS, Hansbro PM, Wark PA. MicroRNA-125a and -b inhibit A20 and MAVS to promote inflammation and impair antiviral response in COPD. *JCI insight* 2017: 2(7): e90443.
17. Liu G, Cooley MA, Jarnicki AG, Hsu AC, Nair PM, Haw TJ, Fricker M, Gellatly SL, Kim RY, Inman MD, Tjin G, Wark PA, Walker MM, Horvat JC, Oliver BG, Argraves WS, Knight DA, Burgess JK, Hansbro PM. Fibulin-1 regulates the pathogenesis of tissue remodeling in respiratory diseases. *JCI insight* 2016: 1(9).

18. Hansbro PM, Hamilton MJ, Fricker M, Gellatly SL, Jarnicki AG, Zheng D, Frei SM, Wong GW, Hamadi S, Zhou S, Foster PS, Krilis SA, Stevens RL. Importance of mast cell Prss31/transmembrane tryptase/tryptase-gamma in lung function and experimental chronic obstructive pulmonary disease and colitis. *The Journal of biological chemistry* 2014: 289(26): 18214-18227.
19. Plank MW, Kaiko GE, Maltby S, Weaver J, Tay HL, Shen W, Wilson MS, Durum SK, Foster PS. Th22 Cells Form a Distinct Th Lineage from Th17 Cells In Vitro with Unique Transcriptional Properties and Tbet-Dependent Th1 Plasticity. *Journal of immunology (Baltimore, Md : 1950)* 2017: 198(5): 2182-2190.
20. Carolan BJ, Heguy A, Harvey BG, Leopold PL, Ferris B, Crystal RG. Up-regulation of expression of the ubiquitin carboxyl-terminal hydrolase L1 gene in human airway epithelium of cigarette smokers. *Cancer research* 2006: 66(22): 10729-10740.
21. Harvey BG, Heguy A, Leopold PL, Carolan BJ, Ferris B, Crystal RG. Modification of gene expression of the small airway epithelium in response to cigarette smoking. *Journal of molecular medicine (Berlin, Germany)* 2007: 85(1): 39-53.
22. Campbell JD, McDonough JE, Zeskind JE, Hackett TL, Pechkovsky DV, Brandsma CA, Suzuki M, Gosselink JV, Liu G, Alekseyev YO, Xiao J, Zhang X, Hayashi S, Cooper JD, Timens W, Postma DS, Knight DA, Lenburg ME, Hogg JC, Spira A. A gene expression signature of emphysema-related lung destruction and its reversal by the tripeptide GHK. *Genome medicine* 2012: 4(8): 67.
23. Fricker M, Deane A, Hansbro PM. Animal models of chronic obstructive pulmonary disease. *Expert opinion on drug discovery* 2014: 9(6): 629-645.
24. Jones B, Donovan C, Liu G, Gomez HM, Chimankar V, Harrison CL, Wiegman CH, Adcock IM, Knight DA, Hirota JA, Hansbro PM. Animal models of COPD: What do they tell us? *Respirology (Carlton, Vic)* 2017: 22(1): 21-32.
25. Starkey MR, Essilfie AT, Horvat JC, Kim RY, Nguyen DH, Beagley KW, Mattes J, Foster PS, Hansbro PM. Constitutive production of IL-13 promotes early-life Chlamydia respiratory infection and allergic airway disease. *Mucosal immunology* 2013: 6(3): 569-579.
26. Starkey MR, Nguyen DH, Essilfie AT, Kim RY, Hatchwell LM, Collison AM, Yagita H, Foster PS, Horvat JC, Mattes J, Hansbro PM. Tumor necrosis factor-related apoptosis-inducing ligand translates neonatal respiratory infection into chronic lung disease. *Mucosal immunology* 2014: 7(3): 478-488.
27. Kedzierski L, Tate MD, Hsu AC, Kolesnik TB, Linossi EM, Dagley L, Dong Z, Freeman S, Infusini G, Starkey MR, Bird NL, Chatfield SM, Babon JJ, Huntington N, Belz G, Webb A, Wark PA, Nicola NA, Xu J, Kedzierska K, Hansbro PM, Nicholson SE. Suppressor of cytokine signaling (SOCS)5 ameliorates influenza infection via inhibition of EGFR signaling. *eLife* 2017: 6.
28. Essilfie AT, Horvat JC, Kim RY, Mayall JR, Pinkerton JW, Beckett EL, Starkey MR, Simpson JL, Foster PS, Gibson PG, Hansbro PM. Macrolide therapy suppresses key features of experimental steroid-sensitive and steroid-insensitive asthma. *Thorax* 2015: 70(5): 458-467.
29. Nair PM, Starkey MR, Haw TJ, Liu G, Horvat JC, Morris JC, Verrills NM, Clark AR, Ammit AJ, Hansbro PM. Targeting PP2A and proteasome activity ameliorates features of allergic airway disease in mice. *Allergy* 2017: 72(12): 1891-1903.
30. Horvat JC, Beagley KW, Wade MA, Preston JA, Hansbro NG, Hickey DK, Kaiko GE, Gibson PG, Foster PS, Hansbro PM. Neonatal chlamydial infection

induces mixed T-cell responses that drive allergic airway disease. *American journal of respiratory and critical care medicine* 2007: 176(6): 556-564.
31. Tam A, Hughes M, McNagny KM, Obeidat M, Hackett TL, Leung JM, Shaipanich T, Dorscheid DR, Singhera GK, Yang CWT, Pare PD, Hogg JC, Nickle D, Sin DD. Hedgehog signaling in the airway epithelium of patients with chronic obstructive pulmonary disease. *Scientific reports* 2019: 9(1): 3353.
32. Horvat JC, Starkey MR, Kim RY, Phipps S, Gibson PG, Beagley KW, Foster PS, Hansbro PM. Early-life chlamydial lung infection enhances allergic airways disease through age-dependent differences in immunopathology. *The Journal of allergy and clinical immunology* 2010: 125(3): 617-625, 625.e611-625.e616.
33. Kim RY, Horvat JC, Pinkerton JW, Starkey MR, Essilfie AT, Mayall JR, Nair PM, Hansbro NG, Jones B, Haw TJ, Sunkara KP, Nguyen TH, Jarnicki AG, Keely S, Mattes J, Adcock IM, Foster PS, Hansbro PM. MicroRNA-21 drives severe, steroid-insensitive experimental asthma by amplifying phosphoinositide 3-kinase-mediated suppression of histone deacetylase 2. *The Journal of allergy and clinical immunology* 2017: 139(2): 519-532.
34. Kim RY, Pinkerton JW, Essilfie AT, Robertson AAB, Baines KJ, Brown AC, Mayall JR, Ali MK, Starkey MR, Hansbro NG, Hirota JA, Wood LG, Simpson JL, Knight DA, Wark PA, Gibson PG, O'Neill LAJ, Cooper MA, Horvat JC, Hansbro PM. Role for NLRP3 Inflammasome-mediated, IL-1beta-Dependent Responses in Severe, Steroid-Resistant Asthma. *American journal of respiratory and critical care medicine* 2017: 196(3): 283-297.
35. Vogelmeier CF, Criner GJ, Martinez FJ, Anzueto A, Barnes PJ, Bourbeau J, Celli BR, Chen R, Decramer M, Fabbri LM, Frith P, Halpin DM, Lopez Varela MV, Nishimura M, Roche N, Rodriguez-Roisin R, Sin DD, Singh D, Stockley R, Vestbo J, Wedzicha JA, Agusti A. Global Strategy for the Diagnosis, Management, and Prevention of Chronic Obstructive Lung Disease 2017 Report. GOLD Executive Summary. *American journal of respiratory and critical care medicine* 2017: 195(5): 557-582.
36. Shan M, Yuan X, Song LZ, Roberts L, Zarinkamar N, Seryshev A, Zhang Y, Hilsenbeck S, Chang SH, Dong C, Corry DB, Kheradmand F. Cigarette smoke induction of osteopontin (SPP1) mediates T(H)17 inflammation in human and experimental emphysema. *Science translational medicine* 2012: 4(117): 117ra119.
37. Aujla SJ, Dubin PJ, Kolls JK. Interleukin-17 in pulmonary host defense. *Experimental lung research* 2007: 33(10): 507-518.
38. Shukla SD, Budden KF, Neal R, Hansbro PM. Microbiome effects on immunity, health and disease in the lung. *Clinical & translational immunology* 2017: 6(3): e133.
39. Budden KF, Shukla SD, Rehman SF, Bowerman KL, Keely S, Hugenholtz P, Armstrong-James DPH, Adcock IM, Chotirmall SH, Chung KF, PM. H. Functional effects of microbiota in chronic respiratory disease. . *Lancet Respiratory Medicine* 2019: In press.
40. Pichavant M, Remy G, Bekaert S, Le Rouzic O, Kervoaze G, Vilain E, Just N, Tillie-Leblond I, Trottein F, Cataldo D, Gosset P. Oxidative stress-mediated iNKT-cell activation is involved in COPD pathogenesis. *Mucosal immunology* 2014: 7(3): 568-578.
41. De Grove KC, Provoost S, Verhamme FM, Bracke KR, Joos GF, Maes T, Brusselle GG. Characterization and Quantification of Innate Lymphoid Cell Subsets in Human Lung. *PloS one* 2016: 11(1): e0145961.

42. Thatcher TH, McHugh NA, Egan RW, Chapman RW, Hey JA, Turner CK, Redonnet MR, Seweryniak KE, Sime PJ, Phipps RP. Role of CXCR2 in cigarette smoke-induced lung inflammation. *American journal of physiology Lung cellular and molecular physiology* 2005: 289(2): L322-328.
43. Meijer M, Rijkers GT, van Overveld FJ. Neutrophils and emerging targets for treatment in chronic obstructive pulmonary disease. *Expert review of clinical immunology* 2013: 9(11): 1055-1068.
44. Li JR, Zhou WX, Huang KW, Jin Y, Gao JM. Interleukin-22 exacerbates airway inflammation induced by short-term exposure to cigarette smoke in mice. *Acta pharmacologica Sinica* 2014: 35(11): 1393-1401.
45. Pociask DA, Scheller EV, Mandalapu S, McHugh KJ, Enelow RI, Fattman CL, Kolls JK, Alcorn JF. IL-22 is essential for lung epithelial repair following influenza infection. *The American journal of pathology* 2013: 182(4): 1286-1296.
46. Wang S, Li Y, Fan J, Zhang X, Luan J, Bian Q, Ding T, Wang Y, Wang Z, Song P, Cui D, Mei X, Ju D. Interleukin-22 ameliorated renal injury and fibrosis in diabetic nephropathy through inhibition of NLRP3 inflammasome activation. *Cell death & disease* 2017: 8(7): e2937.

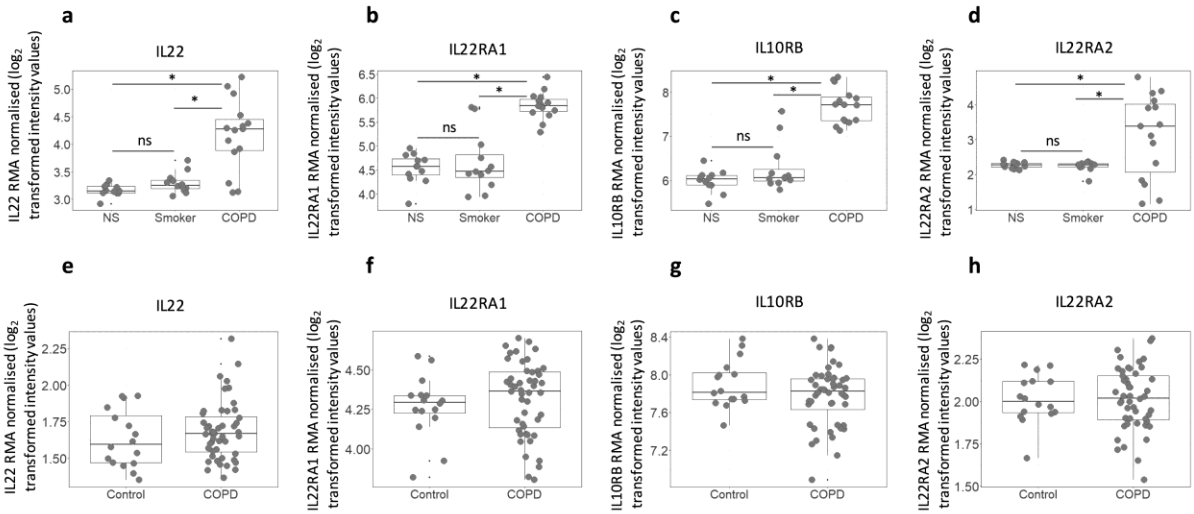
a
IL22
IL22 RMA normalised (log2 transformed intensity values)
ns
*
*
NS
Smoker
COPD
b
IL22RA1
IL22RA1 RMA normalised (log2 transformed intensity values)
c
IL10RB
IL10RB RMA normalised (log2 transformed intensity values)
d
IL22RA2
IL22RA2 RMA normalised (log2 transformed intensity values)
e
IL22
Control
COPD
f
IL22RA1
g
IL10RB
h
IL22RA2

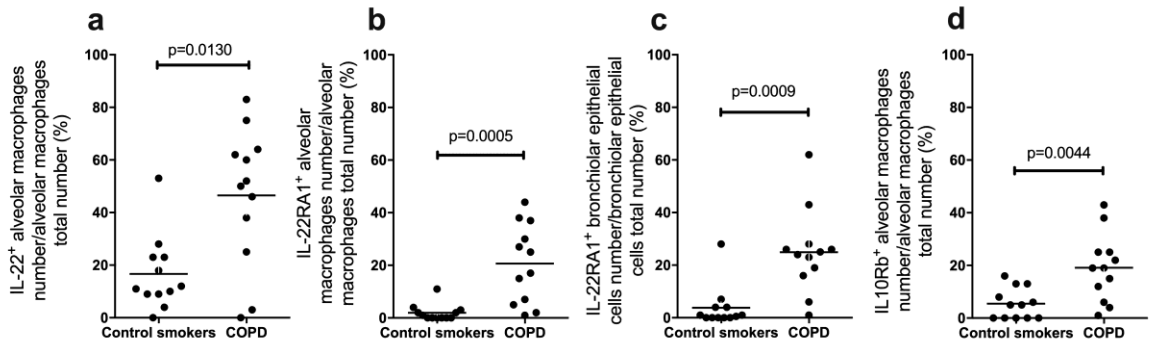
a
b
c
d
IL-22+ alveolar macrophages number/alveolar macrophages total number (%)
IL-22RA1+ alveolar macrophages number/alveolar macrophages total number (%)
IL-22RA1+ bronchiolar epithelial cells number/bronchiolar epithelial cells total number (%)
IL10Rb+ alveolar macrophages number/alveolar macrophages total number (%)
p=0.0130
p=0.0005
p=0.0009
p=0.0044
100
80
60
40
20
0
Control smokers
COPD

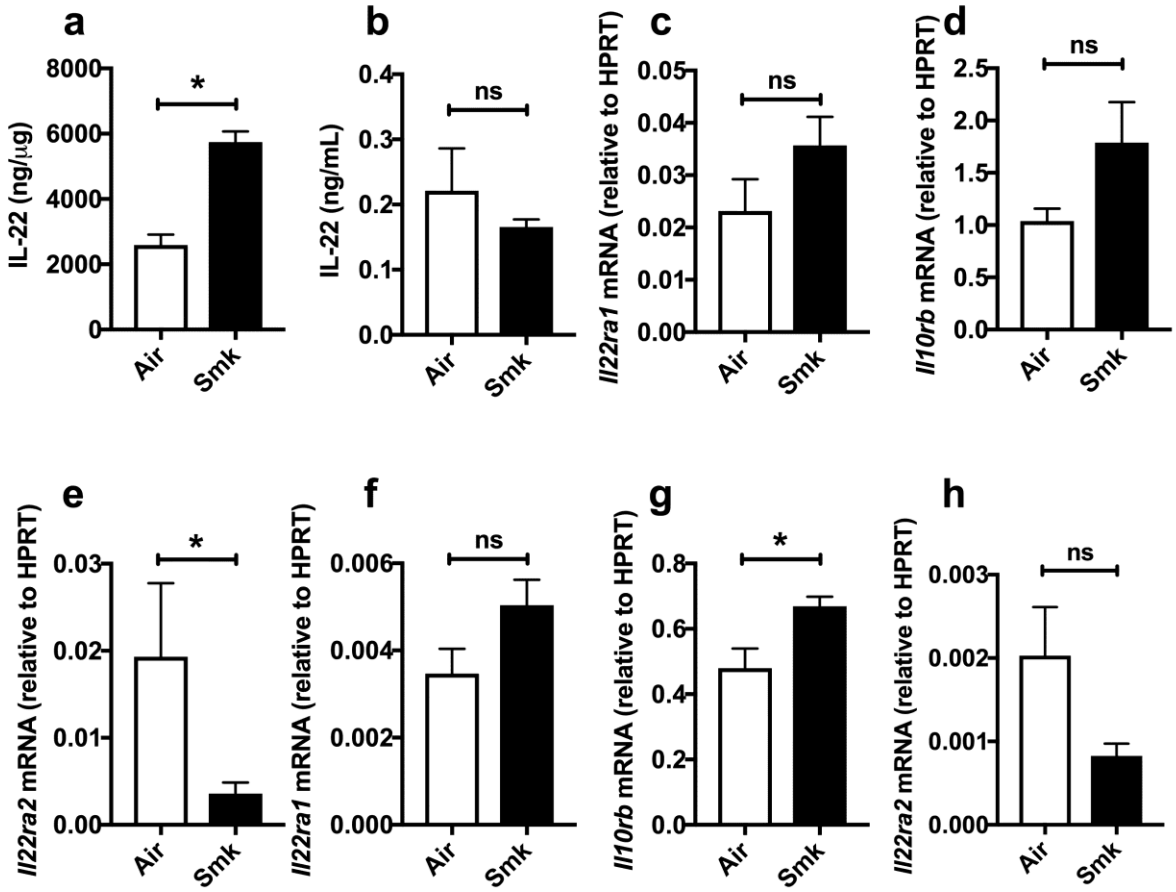
a
IL-22 (ng/μg)
8000
6000
4000
2000
0
*
Air
Smk
b
IL-22 (ng/mL)
0.4
0.3
0.2
0.1
0.0
ns
Air
Smk
c
Il22ra1 mRNA (relative to HPRT)
0.05
0.04
0.03
0.02
0.01
0.00
ns
Air
Smk
d
Il10rb mRNA (relative to HPRT)
2.5
2.0
1.5
1.0
0.5
0.0
ns
Air
Smk
e
Il22ra2 mRNA (relative to HPRT)
0.03
0.02
0.01
0.00
*
Air
Smk
f
Il22ra1 mRNA (relative to HPRT)
0.006
0.004
0.002
0.000
ns
Air
Smk
g
Il10rb mRNA (relative to HPRT)
0.8
0.6
0.4
0.2
0.0
*
Air
Smk
h
Il22ra2 mRNA (relative to HPRT)
0.003
0.002
0.001
0.000
ns
Air
Smk

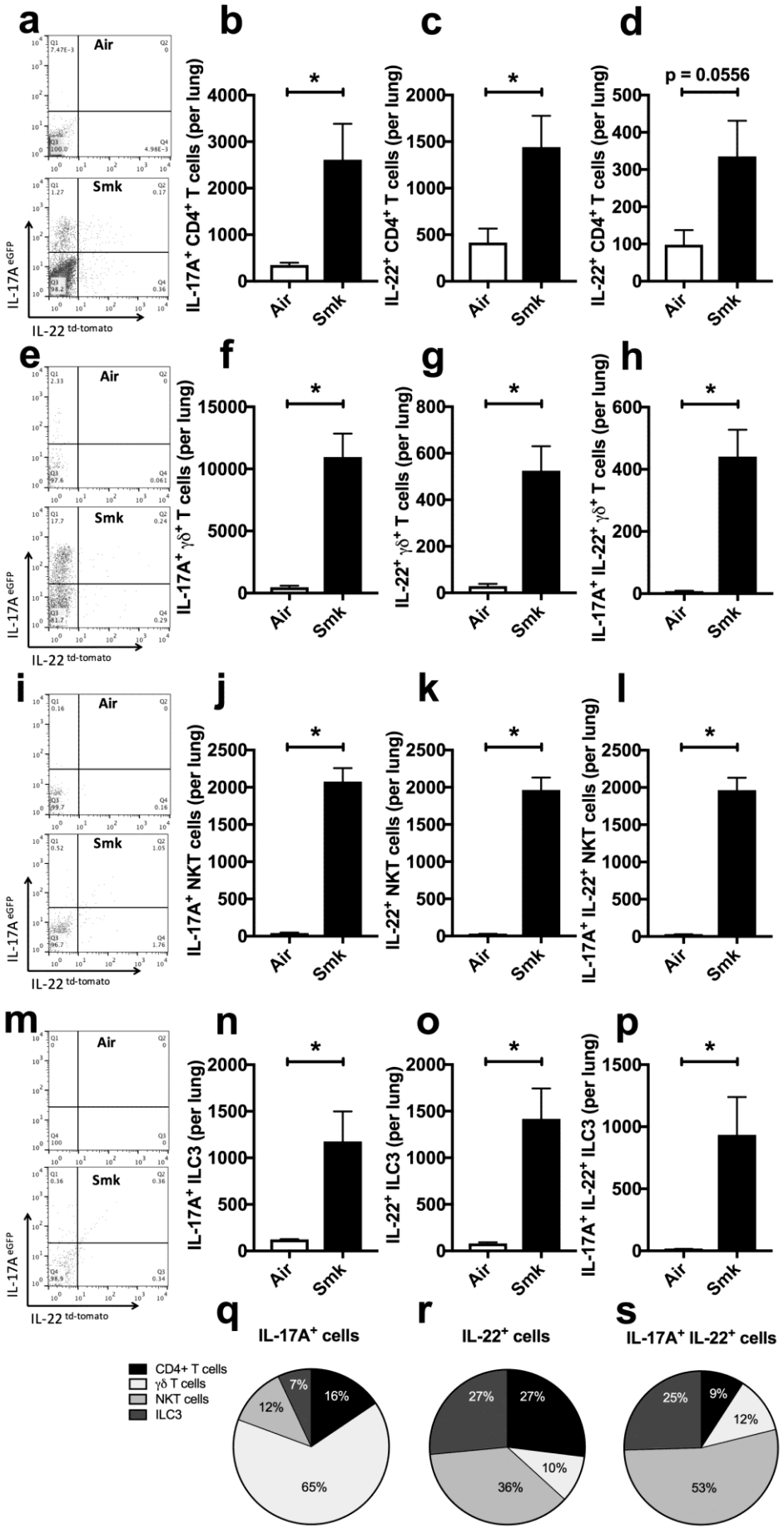
a
Air
Smk
IL-17A eGFP
IL-22 td-tomato
b
IL-17A+ CD4+ T cells (per lung)
c
IL-22+ CD4+ T cells (per lung)
d
p = 0.0556
IL-22+ CD4+ T cells (per lung)
e
IL-17A+ γδ+ T cells (per lung)
f
IL-22+ γδ+ T cells (per lung)
g
IL-17A+ IL-22+ γδ+ T cells (per lung)
h
i
IL-17A+ NKT cells (per lung)
j
IL-22+ NKT cells (per lung)
k
IL-17A+ IL-22+ NKT cells (per lung)
l
m
IL-17A+ ILC3 (per lung)
n
IL-22+ ILC3 (per lung)
o
IL-17A+ IL-22+ ILC3 (per lung)
p
Air
Smk
*
q
IL-17A+ cells
r
IL-22+ cells
s
IL-17A+ IL-22+ cells
CD4+ T cells
γδ T cells
NKT cells
ILC3
16%
7%
12%
65%
27%
27%
10%
36%
25%
9%
12%
53%

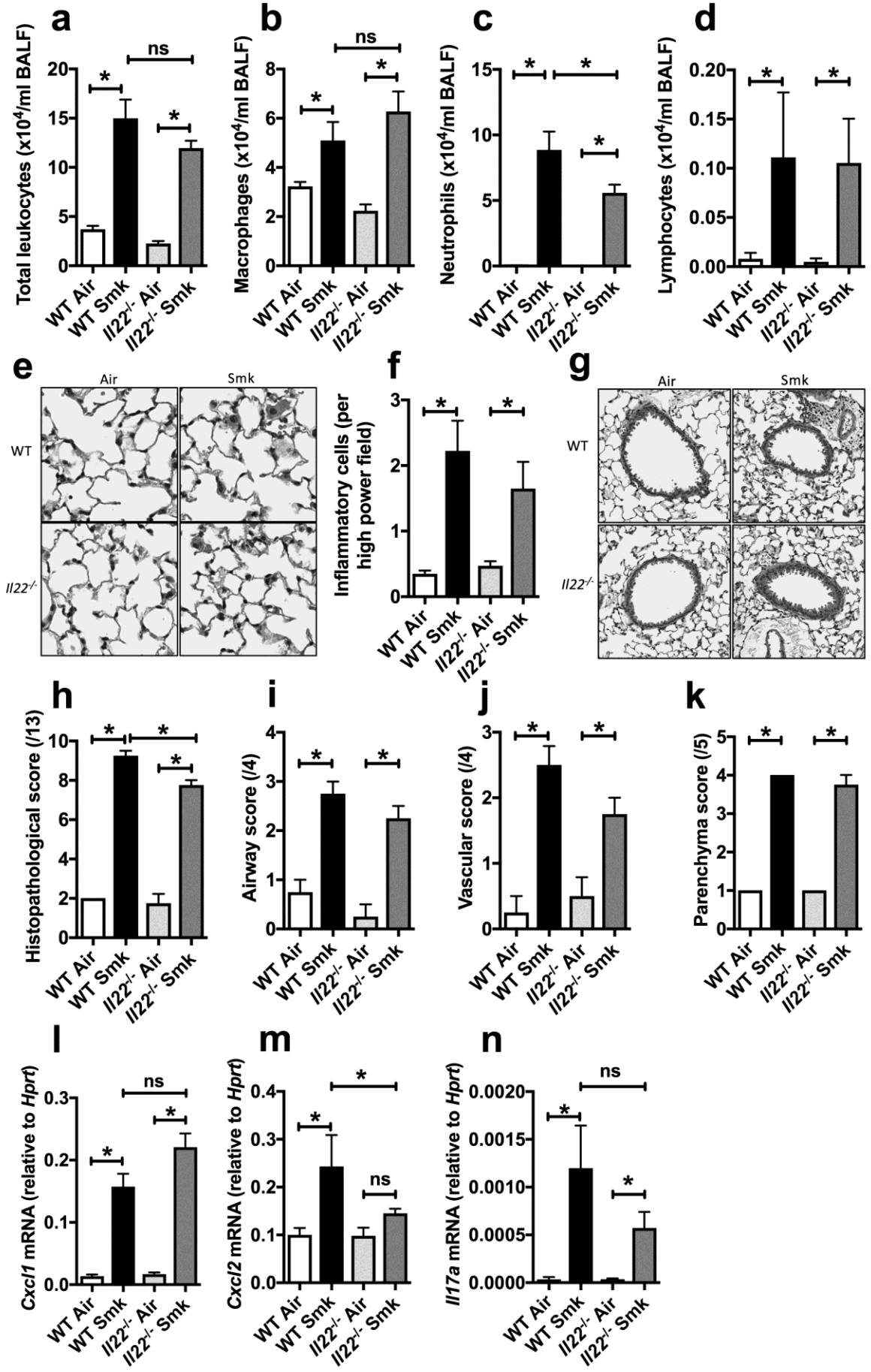
a
Total leukocytes (x10^4/ml BALF)
b
Macrophages (x10^4/ml BALF)
c
Neutrophils (x10^4/ml BALF)
d
Lymphocytes (x10^4/ml BALF)
ns
*
WT Air
WT Smk
Il22-/- Air
Il22-/- Smk
e
Air
Smk
WT
Il22-/-
f
Inflammatory cells (per high power field)
g
h
Histopathological score (/13)
i
Airway score (/4)
j
Vascular score (/4)
k
Parenchyma score (/5)
l
Cxcl1 mRNA (relative to Hprt)
m
Cxcl2 mRNA (relative to Hprt)
n
Il17a mRNA (relative to Hprt)

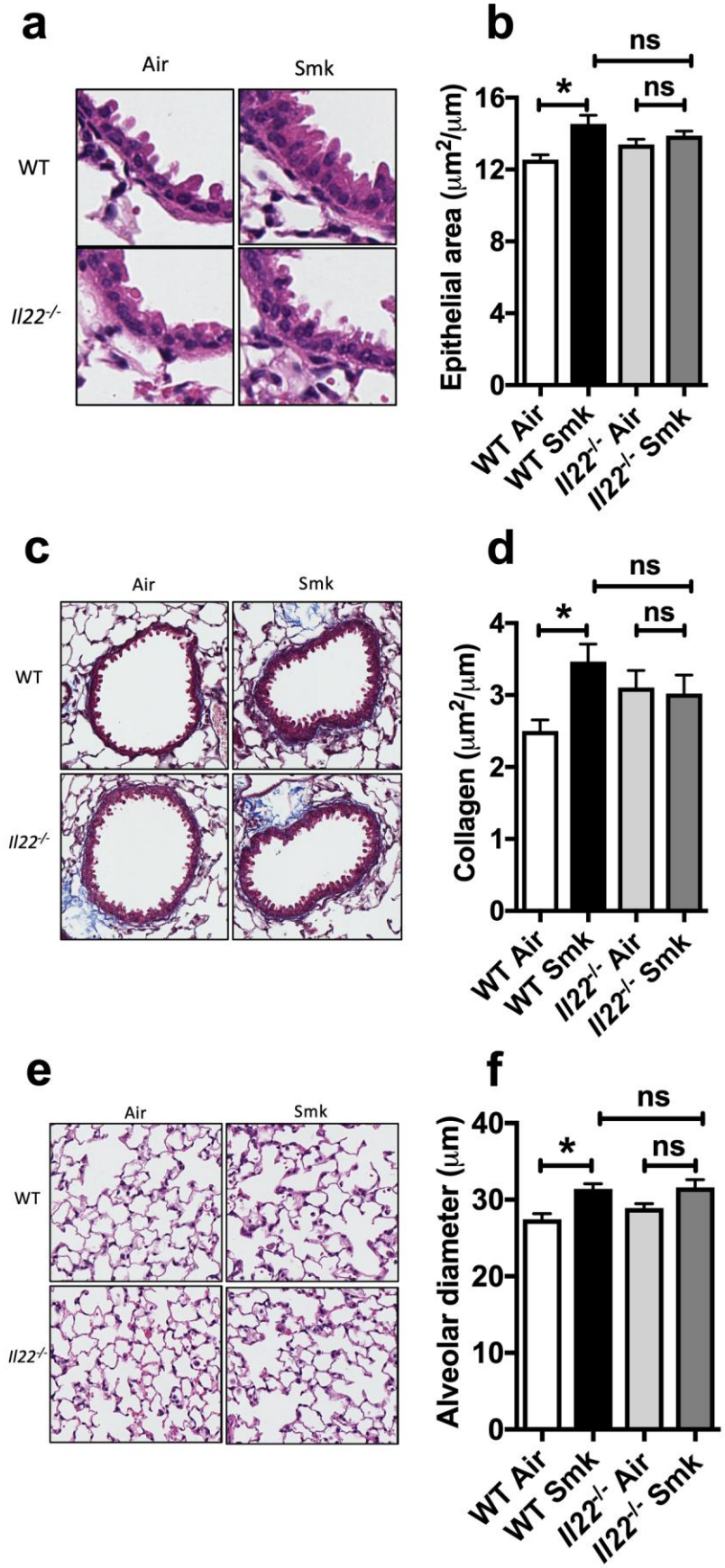
a
Air
Smk
WT
Il22-/-
b
ns
*
ns
Epithelial area (μm2/μm)
16
12
8
4
0
WT Air
WT Smk
Il22-/- Air
Il22-/- Smk
c
Air
Smk
WT
Il22-/-
d
ns
*
ns
Collagen (μm2/μm)
4
3
2
1
0
WT Air
WT Smk
Il22-/- Air
Il22-/- Smk
e
Air
Smk
WT
Il22-/-
f
ns
*
ns
Alveolar diameter (μm)
40
30
20
10
0
WT Air
WT Smk
Il22-/- Air
Il22-/- Smk

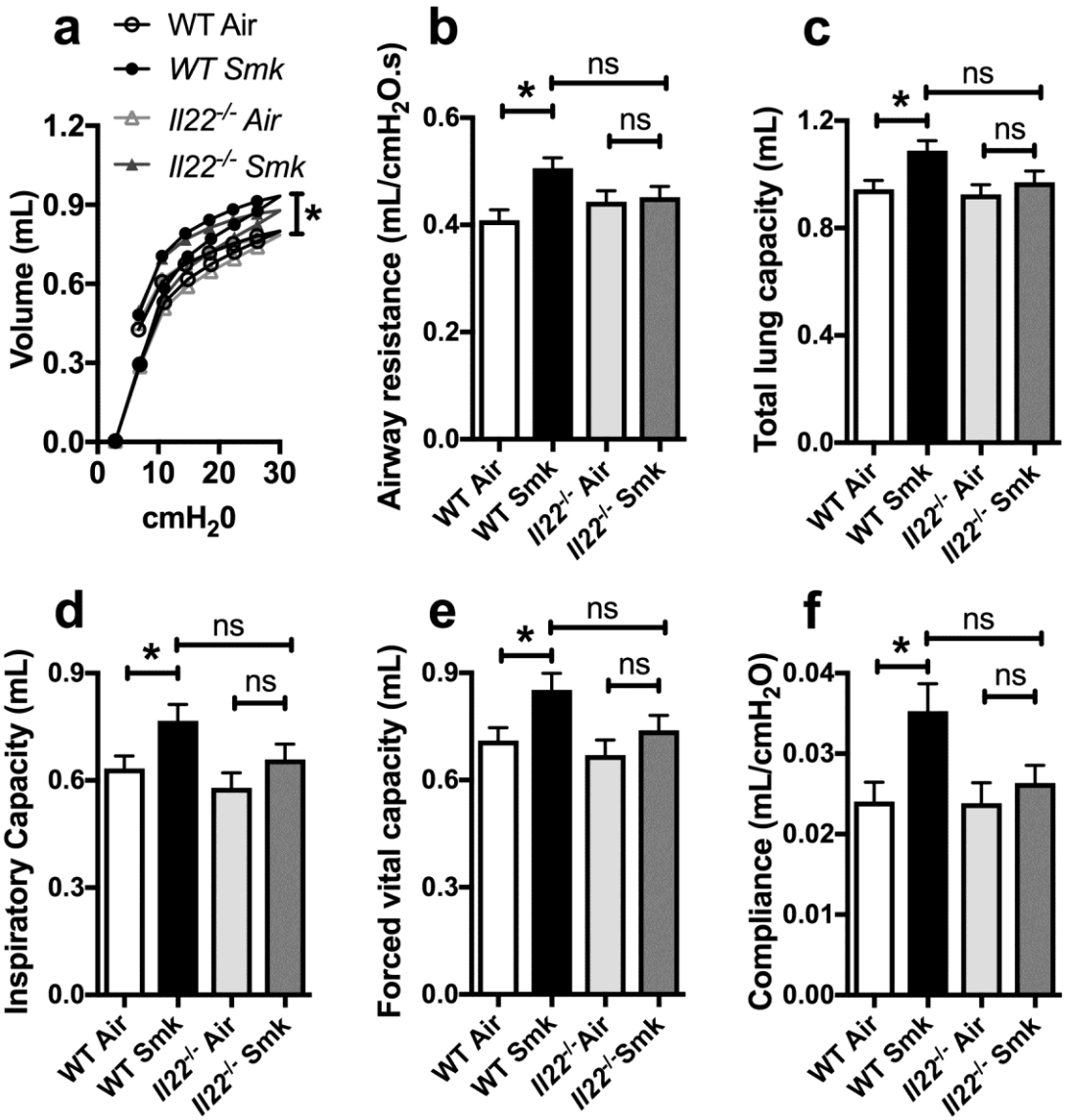
a
WT Air
WT Smk
Il22-/- Air
Il22-/- Smk
Volume (mL)
cmH20
*
b
Airway resistance (mL/cmH2O.s)
c
Total lung capacity (mL)
d
Inspiratory Capacity (mL)
e
Forced vital capacity (mL)
f
Compliance (mL/cmH2O)
ns
WT Air
WT Smk
Il22-/- Air
Il22-/- Smk

IL-22 and its receptors are increased in human and experimental COPD and contribute to pathogenesis

Malcolm R. Starkey[1], Maximilian W. Plank[1], Paolo Casolari[2], Alberto Papi[2], Stelios Pavlidis[3], Yike Guo[3], Guy J.M. Cameron[1], Tatt Jhong Haw[1], Anthony Tam[4,5], Ma'en Obiedat[4,5], Chantal Donovan[1], Nicole G. Hansbro[1,6] Duc H. Nguyen[1], Prema Mono Nair[1], Richard Y. Kim[1], Jay C. Horvat[1], Gerard E. Kaiko[1], Scott K. Durum[5], Peter A. Wark[1], Don D. Sin[4,5], Gaetano Caramori[8], Ian M. Adcock[3], Paul S. Foster[1] and Philip M. Hansbro[1,6]

Affiliations: [1]Priority Research Centre for Healthy Lungs, School of Biomedical Sciences and Pharmacy, Hunter Medical Research Institute & University of Newcastle, Callaghan, New South Wales, Australia. [2]Interdipartimental Study Center for Inflammatory and Smoke-related Airway Diseases (CEMICEF), Cardiorespiratory and Internal Medicine Section, University of Ferrara, Ferrara, Italy. [3]The Airways Disease Section, National Heart & Lung Institute, Imperial College London, London, UK. [4]The University of British Columbia Center for Heart Lung Innovation, St Paul's Hospital, Vancouver, Canada. [5]Respiratory Division, Department of Medicine, University of British Columbia, Vancouver, BC. [6]Centre for inflammation, Centenary Institute, Sydney, and School of Life Sciences, University of Technology, Ultimo, NSW, Australia. [6]Centre for inflammation, Centenary Institute, Sydney, and School of Life Sciences, University of Technology, Ultimo, NSW, Australia. [7]Laboratory of Immunoregulation, Cancer and Inflammation Program, Center for Cancer Research, National Cancer Institute, National Institutes of Health, Frederick, MD, USA. [8]UOC di

Pneumologia, Dipartimento di Scienze Biomediche, Odontoiatriche e delle Immagini Morfologiche e Funzionali (BIOMORF), Università di Messina, Italy.

Correspondence: Professor Philip M. Hansbro, Centre for inflammation, Centenary Institute, Sydney, and School of Life Sciences, University of Technology, Ultimo, NSW, Australia. E-mail: p.hansbro@centenary.org.au

Supplementary methods

Ethics statement. This study was performed in accordance with the recommendations issued by the National Health and Medical Research Council of Australia. All experimental protocols were approved by the animal ethics committee of The University of Newcastle, Australia.

Gene Expression in Human COPD Microarray Datasets. Analysis of IL-22, IL-22RA1 IL-10RB and IL-22RA2 in published human array datasets (Affymetrix Human Genome U133 Plus 2.0 Array, Accession numbers: GSE5058 and GSE27597) [1-3] was performed using the Array Studio software (Omicsoft Corporation, Research Triangle Park, NC, USA) by applying a general linear model adjusting for age and gender and the Benjamini–Hochberg method for p-value adjustment. Data are expressed as $\log_2$ intensity robust multi-array average signals. The Benjamini–Hochberg method for adjusted P value/false discovery rate (FDR) was used to analyse differences between two groups. Statistical significance was set at FDR < 0.05.

In the GSE5058 dataset, gene arrays from small airway epithelial cells obtained from normal non-smokers (n = 12), healthy chronic smokers (n = 12),

smokers with early COPD (n=9), and smokers with established COPD (n = 6) were evaluated. The FEV1/FVC ratio of the subjects in these groups were 99 ± 7, 97 ± 7, 78 ± 4 and 66 ± 14, respectively.

In the GSE27597 dataset, gene arrays from 8 sample pairs from different lung slices from 6 subjects requiring lung transplant for COPD and 2 organ donors were analysed. The 6 subjects with COPD had a FEV1 <25% predicted (severe disease).

In addition, we examined gene expression from lung tissue specimens derived from 56 subjects (GSE8581 [4]). These subjects had undergone lobectomy for removal of a suspected tumour. Tissue was derived from histologically normal tissue distant from the tumour margin. COPD (cases, n = 15) were defined as subjects with FEV1<70% and FEV1/FVC<0.7 and controls (n = 18) as subjects with FEV1>80% and FEV1/FVC>0.7.

Mice. Female, 7-8-week-old, wild-type (WT) C57BL/6, *Il17a*$^{eGFP/+}$;*Il22*$^{td\text{-}tomato/+}$ reporter and *Il22*$^{-/-}$ mice were obtained from the Australian Bioresource Facility, Moss Vale, NSW, Australia. *Il17a*$^{eGFP/+}$*Il22*$^{td\text{-}tomato/+}$ dual reporter and *Il22*$^{-/-}$ and mice were generated as previously described [5]. Mice were housed under a 12-hour light/dark cycle and had free access to food (standard chow) and water. After a period of acclimatization (5 days), mice were randomly placed into experimental groups and exposed to either normal air or nose-only inhalation of CS for eight weeks as described previously [6-13].

Isolation of RNA and qPCR. Total RNA was extracted from whole lung tissue and blunt-dissected airways and parenchyma and reversed transcribed [8]. mRNA

transcripts were determined by real-time quantitative PCR (qPCR, ABIPrism7000, Applied Biosystems, Scoresby, Victoria, Australia) using custom designed primers (Integrated DNA Technologies, Baulkham Hills, New South Wales, Australia), normalized to the reference gene hypoxanthine-guanine phosphoribosyltransferase (*hprt*) (**supplementary table 1**).

Flow Cytometry Analysis. The numbers of IL-17A$^+$ and IL-22$^+$ CD4$^+$ T-cells, $\gamma\delta$ T-cells, NKT-cells and group 3 innate lymphoid cells in lung homogenates were determined based on surface marker expression using flow cytometry (**supplementary table 2**) [14-16]. Flow cytometric analysis was performed using a FACSAriaIII with FACSDiva software (BD Biosciences, North Ryde, Australia). Flow cytometry antibodies were purchased from Biolegend (Karrinyup, Western Australia, Australia) or BD Biosciences (**supplementary table 3**). BD compensation beads (BD Biosciences) were used to compensate for spectral overlap.

Mouse lung IHC. Lungs were perfused, inflated, formalin fixed, paraffin embedded, and sectioned (4µm)[8, 9]. Longitudinal sections of the left lung were deparaffinised by placing on a heating block at 70°C for 15mins then sections were immersed in fresh xylene for 10mins then 5mins. Rehydration was performed using a series of ethanol gradients (100% twice, 90%, 80%, 70%) and 0.85% saline for 5mins each. Heat-induced antigen retrieval was performed in citrate buffer (10mM citric acid, 0.05% Tween 20, pH 6.0) at 100°C for 30mins. Sections were blocked with casein blocker (Thermo Fisher Scientific, Scoresby, Victoria, Australia) for 1h. Sections were washed with PBS-T and incubated overnight at 4°C with either rat anti-Il22ra1

(MAB42941; R&D Systems, Minneapolis, Minnesota, United States) or rabbit anti-Il22ra2 (ab203211; Abcam, Melbourne, Victoria, Australia) antibodies. Following washing with PBS-T, sections were incubated for 30mins at 37°C with either goat anti-rat (HAF005; R&D Systems) or goat-anti-rabbit (ab7090; Abcam) secondary antibodies conjugated to horseradish peroxidase. Each primary and secondary antibody was diluted 1:100 in PBS-T. Following washing with PBS-T, sections were incubated for 20 mins with 3,3'-diaminobenzidine chromogen-substrate buffer (Aligent Technologies, Mulgrave, Victoria, Australia) according to the manufacturer's instructions. Sections were washed with ddH_2O then counterstained with standard haematoxylin for 5mins. Sections were washed with tap H_2O and were dehydrated by immersion in a series of saline, ethanol then xylene, inverse to that described above. Coverslips were mounted with standard non-aqueous medium and slides imaged using a Zeiss Axio microscope with ZEN-blue edition software V2.5 (Carl Zeiss Microscopy, Thornwood, New York, United States). Unless otherwise stated, each incubation was at room temperature protected from light in a humidified chamber. All wash steps were performed 5 times for 3mins each.

Airway remodelling. Airway epithelial (μm^2) and collagen deposition area (μm^2) were assessed in a minimum of four small airways (basement membrane [BM] perimeter <1,000μm) per section [7-9, 12, 13]. Lung sections were stained using Masson's trichrome stain, and photographs of small intact airways were taken at 40x magnification. These photographs were then analysed in ImageJ software (Version 1.50, NIH).

Airway epithelial thickness analysis was performed by carefully tracing the BM and inner epithelial surface perimeters. Airway epithelial area was calculated by

subtracting the inner airway area from the outer airway area. This was then expressed as area per µm of BM.

For collagen analysis, a colour deconvolution method was used to isolate the collagen, stained blue. This method breaks the original photograph into three images, containing three separate colour ranges. In this manner, the blue-stained areas of the images (representing collagen) could be isolated and quantified separately. The BM was traced and measured as described above. Collagen deposition immediately surrounding the airway was traced and measured, but only in images that isolated the blue-stained pixels. We could then reach a quantitative 'collagen per airway' measurement by expressing the area of blue-stained pixels per µm of BM.

Pulmonary Inflammation. Airway inflammation was assessed by differential enumeration of inflammatory cells in bronchoalveolar lavage fluid (BALF) [7, 8, 17-19]. BALF supernatants were stored at -20°C for assessment of IL-22 protein levels. Lung sections were stained with periodic acid-Schiff (PAS) and tissue inflammation assessed by enumeration of inflammatory cells [7, 8, 17, 18]. Histopathological score was determined in lung sections stained with hematoxylin and eosin (H&E) based on established custom-designed criteria [19].

ELISA. Right lung lobes were homogenised on ice in 500uL of PBS supplemented with Complete mini protease inhibitor cocktail (Roche Diagnostic, Sydney, NSW, Australia) and PhosphoSTOP tablets (Roche Diagnostic). Lung homogenates were incubated on ice for 5 mins and subsequently centrifuged (8,000x*g*, 15 mins).

Supernatants were collected, stored at -20°C overnight and total protein levels were determined using Pierce BCA assay kit (Thermo Fisher Scientific) prior to ELISA. IL-17A, IL-22, MPO and neutrophil elastase protein levels were quantified with commercially available ELISA kits (R&D Systems or Biolegend) [5]. IL-22 protein levels were normalised to total protein in lung homogenates.

Lung Function. Mice were anaesthetised with ketamine (100mg/kg) and xylazine (10mg/kg, Troy Laboratories, Smithfield, Australia) prior to tracheostomy. Tracheas were then cannulated and attached to Buxco® Forced Manoeuvres systems apparatus (DSI, St. Paul, Minnesota, USA) to assess total lung capacity [7, 8]. Mice were then attached to a FlexiVent apparatus (FX1 System; SCIREQ, Montreal, Canada) to assess lung volume, airway resistance, inspiratory capacity, forced vital capacity and compliance (tidal volume of 8mL/kg at a respiratory rate of 450 breaths/mins) [7, 20, 21]. All assessments were performed at least three times and the average was calculated for each mouse.

Human lung tissue study population. Peripheral lung samples were obtained from subjects undergoing lung resection for peripheral lung carcinoma from the Respiratory Unit of the University Hospital of Ferrara, Italy (supplementary table 4). Smokers with mild-to-moderate stable COPD (n=12) were compared with age- and smoke history-matched smokers with normal lung function (NLF) (n=12). Diagnosis of COPD was defined according to international guidelines as the presence of post-bronchodilator FEV1/FVC ratio <70% or the presence of cough and sputum production for at least 3 months in each of two consecutive years [22]. All patients were in stable condition at the time of the surgery and had not suffered acute

exacerbations or upper respiratory tract infections in the preceding two months. None had received glucocorticoids or antibiotics within the month preceding surgery, or inhaled bronchodilators within the previous 48 h. Patients had no history of asthma or other allergic diseases. All former smokers had stopped smoking for more than one year. Each patient was subjected to medical history, physical examination, chest radiography, electrocardiogram, routine blood tests, and pulmonary function tests during the week prior to surgery. Pulmonary function tests (Biomedin Spirometer, Padova, Italy) were performed as previously described [23] according to published guidelines.

Lung sample preparation and IHC. Collection, processing, immunohistochemical analysis of lung tissue samples as well as data analysis were performed as previously published [24, 25]. The primary antibodies (anti-human) used are summarised in supplementary table 5. Negative antibody controls used were nonspecific isotype matched Ig at their respective primary antibody concentrations**.** Image analysis was performed [24] using an integrated microscope (Olympus, Albertslund, Denmark), video camera (JVC Digital color, Tatstrup, Denmark), automated microscope stage (Olympus) and PC running Image pro-Plus Software (Media Cybernetics) to quantify the RBP staining areas. Immunostaining counting and interpretation were performed blinded without prior knowledge of clinical-pathologic parameters.

Scoring system for IHC in peripheral lung. Staining analysis was performed as previously published [24, 25]. A bronchiole was taken to be an airway with no

cartilage and glands in its wall. According to a validated method [24] the number of positively stained endoalveolar macrophages was expressed as a percentage of the total cells with the morphological appearance of alveolar macrophages counted inside of the alveoli. The number of bronchiolar epithelial cells with positive staining was expressed as a percentage of the total number of epithelial cells counted in each bronchiolar section and group data were expressed as mean and standard error of the mean (SEM). Airway epithelial-specific IL-22RA1 protein intensity was quantified using the Aperio imaging system and normalized to the length of the basement membrane.

Statistical analyses. Unless otherwise stated, data are presented as means ± standard error of mean (SEM) and are representative of two independent experiments with 6 mice per group. The two-tailed Mann-Whitney test was used to compare two groups. The one-way analysis of variance with Bonferroni post-test was used to compare 3 or more groups. Statistical significance was set at $P < 0.05$ and determined using GraphPad Prism Software version 6 (San Diego, CA, USA).

Supplementary table 1. Custom-designed primers used in qPCR analysis

Primer	**Primer sequence (5' → 3')**
Il22ra1 forward	GTTTTACTACGCCAAGGTCACG
Il22ra1 reverse	CACTTTGGGGATACAGGTCACA
Il10rb forward	ATTCGGAGTGGGTCAATGT
Il10rb reverse	CTGAGAAACGCAGGTGTAAAG
Il22ra2 forward	CTCTTCTGTGACCTGACCAATGA
Il22ra2 reverse	TTATAGTCACGACCGGAGGATCT
Cxcl1 forward	GCTGGGATTCACCTCAAGAA
Cxcl1 reverse	CTTGGGGACACCTTTTAGCA
Cxcl2 forward	TGCTGCTGGCCACCAACCAC
Cxcl2 reverse	AGTGTGACGCCCCCAGGACC
Il17a forward	GTGTCTCTGATGCTGTTGCT
Il17a reverse	GTTGACCTTCACATTCTGGA
Hprt forward	AGGCCAGACTTTGTTGGATTTGAA
Hprt reverse	CAACTTGCGCTCATCTTAGGATTT

Supplementary table 2. Surface antigens used to characterise mouse IL-17A$^+$ IL-22$^+$ lung cell subsets by flow cytometry

Cell subset	Cell surface antigens
CD4$^+$ T cells	CD45$^+$CD3$^+$CD4$^+$CD8$^-$
γδ T cells	CD45$^+$CD3$^+$γδTCR$^+$
NKT cells	CD45$^+$CD3$^+$αGalCer tetramer$^+$
ILC3	CD45$^+$CD3$^-$Ly6C/G$^-$CD11b$^-$B220$^-$TER119$^-$IL-7Rα$^+$CD90.2$^+$
IL-17A and IL-22	Reported by eGFP and td-tomato, respectively

Supplementary table 3. Antibodies used in flow cytometry analysis

Cell surface antigens	Clone	Fluorophore	Company
CD45	30-F11	PerCP-Cy5.5	Biolegend
CD3	17A2	AF700	Biolegend
CD4	RM4-5	APC-Cy7	Biolegend
CD8	53-6.7	BV510	Biolegend
γδTCR	GL3	BV421	Biolegend
αGalCer Tetramer	N/A	BV605	N/A
Lineage cocktail (CD3, Ly6C/G, CD11b, B220, TER119)	17A2, RB6-8C5, M1/70, RA3-6B2, Ter-119	AF700	Biolegend

Supplementary Table 4. Characteristics of subjects for the immunohistochemical study of interleukins on peripheral lung

Subjects	N.	Age	Sex	Smoking history	Pack-years	Chronic bronchitis	FEV_1 % pred	FEV_1/ FVC %
Control smokers	12	70.8 ±2.3	10M/ 2F	8 Ex smokers 4 Current smokers	41.9 ±11.4	0	104.3±4.0	76.7±1.3
COPD	12	72.4 ±1.5	12M	7 Ex smokers 5 Current smokers	40.6 ±3.3	4 with chronic bronchitis	76.9±6.2	61.6±2.7

Supplementary table 5. Primary antibodies and immunohistochemical conditions used for identification of interleukins in the peripheral lung

Antigen	Company	Catalogue	Host	Concentration	Secondary antibody
IL10Rb	MyBio Source	MBS2003603	Rabbit	1.8 µg/ml	Goat anti-rabbit IgG, Vector (BA 1000); 1:200
IL-22	R&D	AF782	Goat	4 µg/ml	Rabbit anti-goat IgG, Vector (BA 5000); 1:200
IL22RA1 / IL22R	EMD Millipore/LSBio	06-1077-I/LS-B1365	Rabbit	2.2 µg/ml	Goat anti-rabbit IgG, Vector (BA 1000); 1:200
IL22RA2	Atlas	HPA030582	Rabbit	1 µg/ml	Goat anti-rabbit IgG, Vector (BA 1000); 1:200

Supplementary table 6. Immunohistochemical percentage of peripheral lung IL-22-positive cells

Localization and antigen	Control smokers	COPD	Mann-Whitney test p value
Bronchiolar epithelium			
Nuclear	8.3±2.8	9.0±2.5	0.6427
	5.0 (9.6)	5.0 (8.7)	
	1.0-13.8	2.0-18.0	
Cytosolic	48.5±7.0	60.8±6.6	0.2037
	54.5 (24.1)	67.5 (22.8)	
	25.3-70.3	44.5-76.3	
Alveolar macrophages			
Nuclear	16.7±4.1	46.5±7.5	0.0130
	11.5 (14.1)	51.0 (26.1)	
Cytosolic	9.0-23.0	28.3-63.5	0.0602
	62.0 (20.3)	58.0 (13.8)	

	40.8-76.5	27.0-48.5	

Data expressed as mean ± SEM (first line), median (SD) (second line) and interquartile range (third line). Data expressed as mean ± SEM (first line), median (SD) (second line) and interquartile range (third line).

Supplementary table 7. Immunohistochemical percentage of peripheral lung IL22RA1-positive cells

Localization and antigen	**Control smokers**	**COPD**	**Mann-Whitney test p value**
Bronchiolar epithelium			
Nuclear	3.8±2.3	24.9±4.6	0.0009
	0.8 (7.9)	24.5 (15.9)	
	0.0-4.0	16.8-27.5	
Cytosolic	30.5±7.8	8.2±3.5	0.0123
	21.5 (27.1)	2.0 (12.1)	
	7.0-57.3	0.0-16.8	
Alveolar macrophages			
Nuclear	1.9±0.9	20.7±4.3	0.0005
	0.5 (3.2)	21.0 (15.0)	
	0.0-2.8	5.5-35.3	
Cytosolic	0.0-2.8	5.5-35.3	0.0022
	72.5±3.9	52.0±3.9	
	75.0 (13.4)	49.0 (13.5)	

Data expressed as mean ± SEM (first line), median (SD) (second line) and interquartile range (third line). Data expressed as mean ± SEM (first line), median (SD) (second line) and interquartile range (third line).

Supplementary table 8. Immunohistochemical percentage of peripheral lung IL22RA2-positive cells

Localization and antigen	**Control smokers**	**COPD**	**Mann-Whitney test p value**
Bronchiolar epithelium			

Nuclear	0	0	-----
	0	0	
	0	0	
Cytosolic	25.7±7.0	11.8±3.7	0.1645
	19.0 (24.1)	8.0 (12.8)	
	3.5-49.5	1.3-20.5	
Alveolar macrophages			
Nuclear	0	0	-----
	0	0	
	0	0	
Cytosolic	47.5±5.0	48.2±8.5	0.8173
	46.5 (17.5)	52.5 (29.3)	
	34.3-59.8	22.5-73.3	

Data expressed as mean ± SEM (first line), median (SD) (second line) and interquartile range (third line). Data expressed as mean ± SEM (first line), median (SD) (second line) and interquartile range (third line).

Supplementary table 9. Immunohistochemical percentage of peripheral lung IL10Rb-positive cells

Localization and antigen	**Control smokers**	**COPD**	**Mann-Whitney test p value**
Bronchiolar epithelium			
Nuclear	1.8±0.8	3.4±1.1	0.1259
	0.5 (2.6)	2.0 (3.8)	
	0.0-2.8	1.0-4.8	
Cytosolic	27.0±7.6	26.9±5.3	0.7505
	16.0 (26.5)	18.5 (18.4)	
	2.8-58.3	13.0-41.8	
Alveolar macrophages			
Nuclear	5.5±1.7	19.1±3.7	0.0044
	5.0 (5.9)	19.0 (12.8)	

	0.0-11.8	7.5-25.0	
Cytosolic	59.8±5.9	59.6±4.0	0.9769
	62.0 (20.3)	58.0 (13.8)	
	38.5-76.5	49.3-66.8	

Data expressed as mean ± SEM (first line), median (SD) (second line) and interquartile range (third line).

Supplementary Table 10. Characteristics of subjects for the IL-22RA1 intensity in airway epithelial cells

Subjects	**Non-smokers**	**Healthy smokers**	**GOLD 2**	**GOLD 3, 4**
Sex (M/F)	2/4	2/4	6/3	4/5
Smoking status (current/ex/NA)	0/0/0	4/2/0	4/3/2	1/8/0
Age (mean ± SD)	58.0±18.1	65.8±9.2	63.7±9.0	60.3±6.0
FEV1/FVC % (mean ± SD)	82.9±4.4	76.5±3.5	57.1±5.6	33.5±11.1

References

1. Carolan BJ, Heguy A, Harvey BG, Leopold PL, Ferris B, Crystal RG. Up-regulation of expression of the ubiquitin carboxyl-terminal hydrolase L1 gene in human airway epithelium of cigarette smokers. *Cancer research* 2006: 66(22): 10729-10740.
2. Harvey BG, Heguy A, Leopold PL, Carolan BJ, Ferris B, Crystal RG. Modification of gene expression of the small airway epithelium in response to cigarette smoking. *Journal of molecular medicine (Berlin, Germany)* 2007: 85(1): 39-53.
3. Campbell JD, McDonough JE, Zeskind JE, Hackett TL, Pechkovsky DV, Brandsma CA, Suzuki M, Gosselink JV, Liu G, Alekseyev YO, Xiao J, Zhang X, Hayashi S, Cooper JD, Timens W, Postma DS, Knight DA, Lenburg ME, Hogg JC, Spira A. A gene expression signature of emphysema-related lung destruction and its reversal by the tripeptide GHK. *Genome medicine* 2012: 4(8): 67.
4. Bhattacharya S, Srisuma S, Demeo DL, Shapiro SD, Bueno R, Silverman EK, Reilly JJ, Mariani TJ. Molecular biomarkers for quantitative and discrete COPD phenotypes. *American journal of respiratory cell and molecular biology* 2009: 40(3): 359-367.
5. Plank MW, Kaiko GE, Maltby S, Weaver J, Tay HL, Shen W, Wilson MS, Durum SK, Foster PS. Th22 Cells Form a Distinct Th Lineage from Th17 Cells In Vitro with Unique Transcriptional Properties and Tbet-Dependent Th1 Plasticity. *Journal of immunology (Baltimore, Md : 1950)* 2017: 198(5): 2182-2190.
6. Fricker M GB, Mateer S, Jones B, Kim RY, Gellatly SL, Jarnicki AG, Powell N, Oliver BG, Radford-Smith G, Talley NJ, Walker MM, Keely S, Hansbro PM. . Chronic smoke exposure induces systemic hypoxia that drives intestinal dysfunction. . *JCI insight* 2018(In Press).
7. Beckett EL, Stevens RL, Jarnicki AG, Kim RY, Hanish I, Hansbro NG, Deane A, Keely S, Horvat JC, Yang M, Oliver BG, van Rooijen N, Inman MD, Adachi R, Soberman RJ, Hamadi S, Wark PA, Foster PS, Hansbro PM. A new short-term mouse model of chronic obstructive pulmonary disease identifies a role for mast cell tryptase in pathogenesis. *The Journal of allergy and clinical immunology* 2013: 131(3): 752-762.
8. Haw TJ, Starkey MR, Pavlidis S, Fricker M, Arthurs AL, Mono Nair P, Liu G, Hanish I, Kim RY, Foster PS, Horvat JC, Adcock IM, Hansbro PM. Toll-like receptor 2 and 4 have Opposing Roles in the Pathogenesis of Cigarette Smoke-induced Chronic Obstructive Pulmonary Disease. *American journal of physiology Lung cellular and molecular physiology* 2017: ajplung.00154.02017.
9. Haw TJ, Starkey MR, Nair PM, Pavlidis S, Liu G, Nguyen DH, Hsu AC, Hanish I, Kim RY, Collison AM, Inman MD, Wark PA, Foster PS, Knight DA, Mattes J, Yagita H, Adcock IM, Horvat JC, Hansbro PM. A pathogenic role for tumor necrosis factor-related apoptosis-inducing ligand in chronic obstructive pulmonary disease. *Mucosal immunology* 2016: 9(4): 859-872.
10. Hsu AC, Starkey MR, Hanish I, Parsons K, Haw TJ, Howland LJ, Barr I, Mahony JB, Foster PS, Knight DA, Wark PA, Hansbro PM. Targeting PI3K-p110alpha Suppresses Influenza Virus Infection in Chronic Obstructive Pulmonary Disease. *American journal of respiratory and critical care medicine* 2015: 191(9): 1012-1023.
11. Hsu AC, Dua K, Starkey MR, Haw TJ, Nair PM, Nichol K, Zammit N, Grey ST, Baines KJ, Foster PS, Hansbro PM, Wark PA. MicroRNA-125a and -b inhibit A20

and MAVS to promote inflammation and impair antiviral response in COPD. *JCI insight* 2017: 2(7): e90443.
12. Liu G, Cooley MA, Jarnicki AG, Hsu AC, Nair PM, Haw TJ, Fricker M, Gellatly SL, Kim RY, Inman MD, Tjin G, Wark PA, Walker MM, Horvat JC, Oliver BG, Argraves WS, Knight DA, Burgess JK, Hansbro PM. Fibulin-1 regulates the pathogenesis of tissue remodeling in respiratory diseases. *JCI insight* 2016: 1(9).
13. Hansbro PM, Hamilton MJ, Fricker M, Gellatly SL, Jarnicki AG, Zheng D, Frei SM, Wong GW, Hamadi S, Zhou S, Foster PS, Krilis SA, Stevens RL. Importance of mast cell Prss31/transmembrane tryptase/tryptase-gamma in lung function and experimental chronic obstructive pulmonary disease and colitis. *The Journal of biological chemistry* 2014: 289(26): 18214-18227.
14. Starkey MR, Nguyen DH, Essilfie AT, Kim RY, Hatchwell LM, Collison AM, Yagita H, Foster PS, Horvat JC, Mattes J, Hansbro PM. Tumor necrosis factor-related apoptosis-inducing ligand translates neonatal respiratory infection into chronic lung disease. *Mucosal immunology* 2014: 7(3): 478-488.
15. Starkey MR, Essilfie AT, Horvat JC, Kim RY, Nguyen DH, Beagley KW, Mattes J, Foster PS, Hansbro PM. Constitutive production of IL-13 promotes early-life Chlamydia respiratory infection and allergic airway disease. *Mucosal immunology* 2013: 6(3): 569-579.
16. Kedzierski L, Tate MD, Hsu AC, Kolesnik TB, Linossi EM, Dagley L, Dong Z, Freeman S, Infusini G, Starkey MR, Bird NL, Chatfield SM, Babon JJ, Huntington N, Belz G, Webb A, Wark PA, Nicola NA, Xu J, Kedzierska K, Hansbro PM, Nicholson SE. Suppressor of cytokine signaling (SOCS)5 ameliorates influenza infection via inhibition of EGFR signaling. *eLife* 2017: 6.
17. Essilfie AT, Horvat JC, Kim RY, Mayall JR, Pinkerton JW, Beckett EL, Starkey MR, Simpson JL, Foster PS, Gibson PG, Hansbro PM. Macrolide therapy suppresses key features of experimental steroid-sensitive and steroid-insensitive asthma. *Thorax* 2015: 70(5): 458-467.
18. Nair PM, Starkey MR, Haw TJ, Liu G, Horvat JC, Morris JC, Verrills NM, Clark AR, Ammit AJ, Hansbro PM. Targeting PP2A and proteasome activity ameliorates features of allergic airway disease in mice. *Allergy* 2017: 72(12): 1891-1903.
19. Horvat JC, Beagley KW, Wade MA, Preston JA, Hansbro NG, Hickey DK, Kaiko GE, Gibson PG, Foster PS, Hansbro PM. Neonatal chlamydial infection induces mixed T-cell responses that drive allergic airway disease. *American journal of respiratory and critical care medicine* 2007: 176(6): 556-564.
20. Kim RY, Horvat JC, Pinkerton JW, Starkey MR, Essilfie AT, Mayall JR, Nair PM, Hansbro NG, Jones B, Haw TJ, Sunkara KP, Nguyen TH, Jarnicki AG, Keely S, Mattes J, Adcock IM, Foster PS, Hansbro PM. MicroRNA-21 drives severe, steroid-insensitive experimental asthma by amplifying phosphoinositide 3-kinase-mediated suppression of histone deacetylase 2. *The Journal of allergy and clinical immunology* 2017: 139(2): 519-532.
21. Kim RY, Pinkerton JW, Essilfie AT, Robertson AAB, Baines KJ, Brown AC, Mayall JR, Ali MK, Starkey MR, Hansbro NG, Hirota JA, Wood LG, Simpson JL, Knight DA, Wark PA, Gibson PG, O'Neill LAJ, Cooper MA, Horvat JC, Hansbro PM. Role for NLRP3 Inflammasome-mediated, IL-1beta-Dependent Responses in Severe, Steroid-Resistant Asthma. *American journal of respiratory and critical care medicine* 2017: 196(3): 283-297.
22. Kirkham PA, Caramori G, Casolari P, Papi AA, Edwards M, Shamji B, Triantaphyllopoulos K, Hussain F, Pinart M, Khan Y, Heinemann L, Stevens L, Yeadon M, Barnes PJ, Chung KF, Adcock IM. Oxidative stress-induced antibodies to

carbonyl-modified protein correlate with severity of chronic obstructive pulmonary disease. *American journal of respiratory and critical care medicine* 2011: 184(7): 796-802.
23. Marwick JA, Caramori G, Casolari P, Mazzoni F, Kirkham PA, Adcock IM, Chung KF, Papi A. A role for phosphoinositol 3-kinase delta in the impairment of glucocorticoid responsiveness in patients with chronic obstructive pulmonary disease. *The Journal of allergy and clinical immunology* 2010: 125(5): 1146-1153.
24. Caramori G, Adcock IM, Casolari P, Ito K, Jazrawi E, Tsaprouni L, Villetti G, Civelli M, Carnini C, Chung KF, Barnes PJ, Papi A. Unbalanced oxidant-induced DNA damage and repair in COPD: a link towards lung cancer. *Thorax* 2011: 66(6): 521-527.
25. Tam A, Hughes M, McNagny KM, Obeidat M, Hackett TL, Leung JM, Shaipanich T, Dorscheid DR, Singhera GK, Yang CWT, Pare PD, Hogg JC, Nickle D, Sin DD. Hedgehog signaling in the airway epithelium of patients with chronic obstructive pulmonary disease. *Scientific reports* 2019: 9(1): 3353.

Supplementary figure legends

Supplementary Figure 1: Gating strategy for lung immune cell subsets. (**a**) $CD4^+$ T cells, (**b**) $\gamma\delta$ T cells and NKT cells and (**c**) ILC3.

Supplementary Figure 2: IL-22 and receptor mRNA in human peripheral lung tissue is unchanged in mild emphysema. Microarray data from peripheral lung tissue of patients with mild emphysema (Accession: GSE8581). (**a**) IL-22, (**b**) IL-22RA1, (**c**) IL-22RA1 and (**d**) IL-10RB. Data are represented as $\log_2$ intensity robust multi-array average signals.

Supplementary Figure 3: No correlation between smoking pack-years and IL-22 or receptor expression. (**a**) IL-22, (**b**) IL-22RA1, (**c**) IL-22RA2

Supplementary Figure 4: No change in IL-22 or receptors in bronchial brushings in lung cancer. Microarray data from bronchial brushings in lung cancer (Accession: GSE4115). (**a**) IL-22, (**b**) IL-22RA1, (**c**) IL-10RB. Data are represented as $\log_2$ intensity robust multi-array average signals.

Supplementary Figure 5: No change in IL-22 or receptors in lung tissue in lung cancer. Microarray data from lung tissue in lung cancer (Accession: GSE1650). (**a**) IL-22, (**b**) IL-22RA1, (**c**) IL-10RB. Data are represented as $\log_2$ intensity robust multi-array average signals.

Supplementary figure 6: Representative images of IL-22 and IL-22 receptor staining in human lung tissue. The four panels are showing the representative images of IL-22 (upper panel), IL-22RA1 (upper middle panel), IL-22RA2 (lower middle panel) and IL-10RB (lower panel) immunohistochemical staining in human peripheral lung tissue. (**a and d**) represent age- and smoke history-matched control smokers with normal lung function and (**b and e**) represent mild-to-moderate stable COPD. Upper lane images show the bronchiolar epithelium whereas lower lanes the alveolar macrophages. Representative images of positive control tissues (tonsils for IL-22, IL-22RA1 and IL-10RB), normal kidney for IL-22RA2 (kindly provided respectively by Prof Stefano Pelucchi and Prof Carmelita Di Gregorio) were stained with primary antibody (**c**) or with nonspecific immunoglobulin (Ig)G (negative control, **f**). Total magnification: 1000x (**a, b, d, e**; bar = 20 μm) or 200x (**c, f**; bar = 100 μm).

Supplementary figure 7: Increased IL-22RA1 protein intensity in the airway epithelium of smokers with COPD. (**a**) IL-22RA1 protein intensity per micrometre (μm) of basement membrane (BM) in non-smokers, healthy smokers without COPD and COPD with or without current smoking separated into GOLD stage 2 and GOLD stage 3-4. (**b**) IL-22RA1 intensity in airway epithelium of non-smokers vs. smokers with COPD. (**c**) Representative images of IL-22RA1 positive staining, with red staining in the airway epithelial cells indicating IL-22RA1 positive staining.

Supplementary figure 8: IL-22 protein levels are unaltered in the lungs of mice exposed to CS for 1 week. Wild-type (WT) C57BL/6 mice were exposed to normal air or CS for 1 week. IL-22 protein levels in lung homogenates were assessed by ELISA. Data are presented as mean ± SEM, n = 6, with another independent experiment showing similar results. Two-tailed Mann-Whitney t-test was used to analyse differences between two groups.

Supplementary figure 9: Representative images of IL-22RA1 and IL-22RA2 protein in mouse lung tissue sections. Wild-type (WT) C57BL/6 mice were exposed to normal air or CS for 8 weeks. Representative images of negative control (top row), IL-22RA1 and IL-22RA2 staining in mouse lung tissue sections from normal air- (left) and CS-exposed (right) mice.

Supplementary figure 10: IL-17A, MPO and neutrophil elastase protein levels are increased in experimental COPD, but not in the absence of IL-22. Wild-type (WT) and IL-22-deficient (*Il22*$^{-/-}$) C57BL/6 mice were exposed to normal air or CS for

8 weeks to induce experimental COPD. (**a**) IL-17A, (**b**) MPO and (**c**) neutrophil elastase protein levels in lung homogenates. Data are presented as mean ± SEM, n = 6, with another independent experiment showing similar results. The one-way analysis of variance with Bonferroni post-test analysed differences between 3 or more groups, whereby * = $p<0.05$ compared to normal air-exposed controls. ns = not significant.

Supplementary Figure 11: CS induced non-significant reductions in tissue elastance that was not different in *Il22*$^{-/-}$ mice. Wild-type (WT) and IL-22-deficient (*Il22*$^{-/-}$) C57BL/6 mice were exposed to normal air or CS for 8 weeks to induce experimental COPD. Lung function was assessed in terms of tissue elastance. Data are presented as mean ± SEM, n = 6, with another independent experiment showing similar results. The one-way analysis of variance with Bonferroni post-test analysed differences between 3 or more groups. ns = not significant.

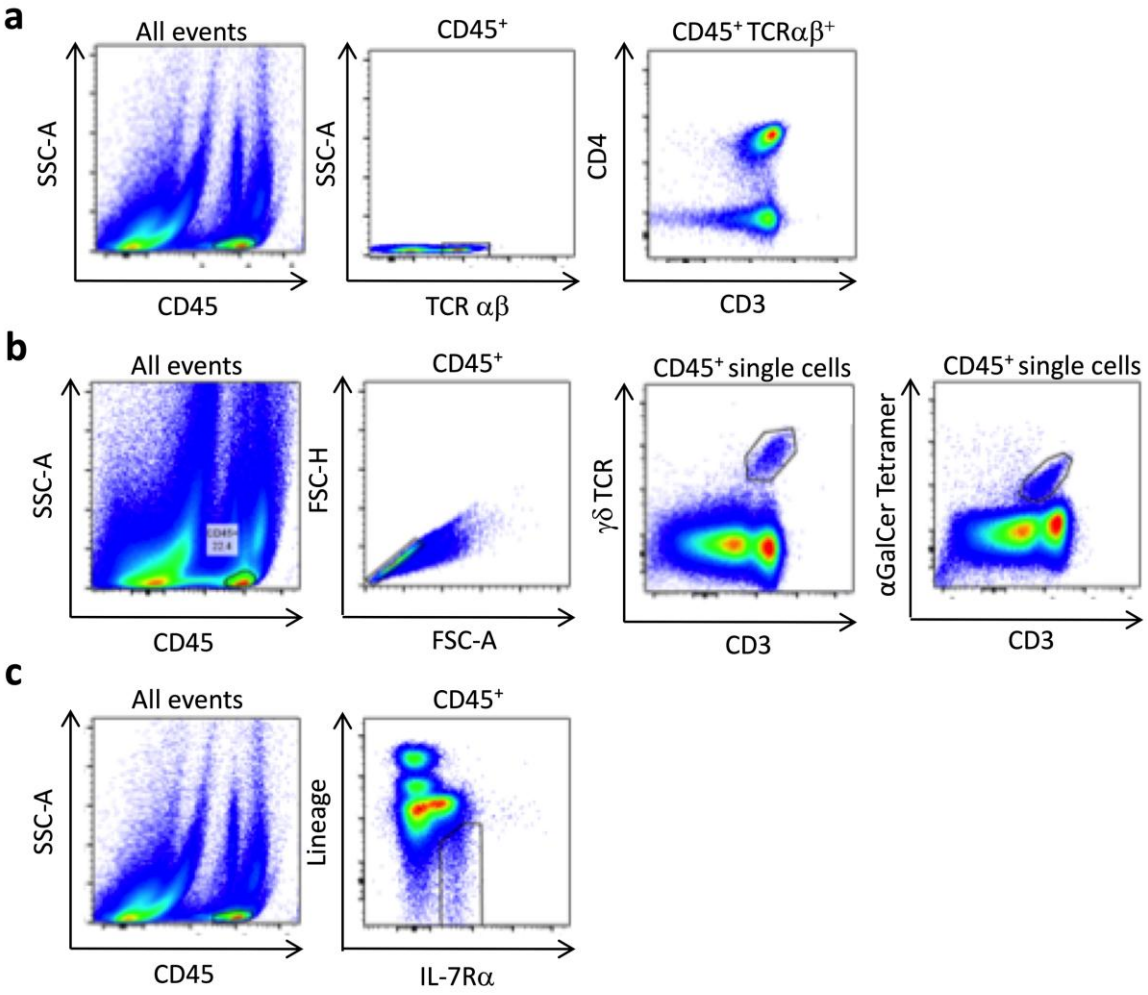
a
All events
SSC-A
CD45
CD45+
SSC-A
TCR αβ
CD45+ TCRαβ+
CD4
CD3
b
All events
SSC-A
CD45
CD45+
FSC-H
FSC-A
CD45+ single cells
γδ TCR
CD3
CD45+ single cells
αGalCer Tetramer
CD3
c
All events
SSC-A
CD45
CD45+
Lineage
IL-7Rα

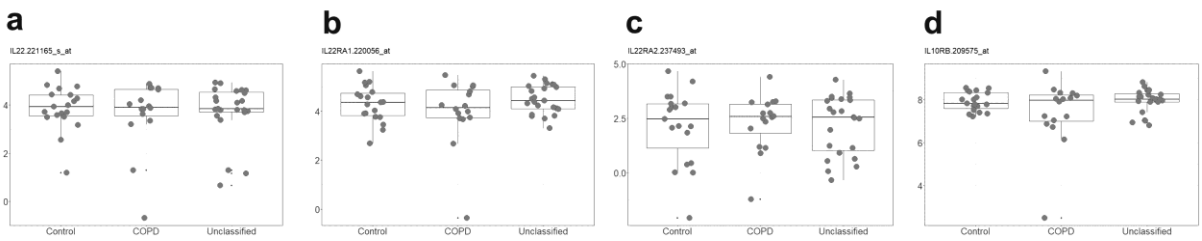
a
IL22.221165_s_at
4
2
0
Control
COPD
Unclassified
b
IL22RA1.220056_at
4
2
0
Control
COPD
Unclassified
c
IL22RA2.237493_at
5.0
2.5
0.0
Control
COPD
Unclassified
d
IL10RB.209575_at
8
6
4
Control
COPD
Unclassified

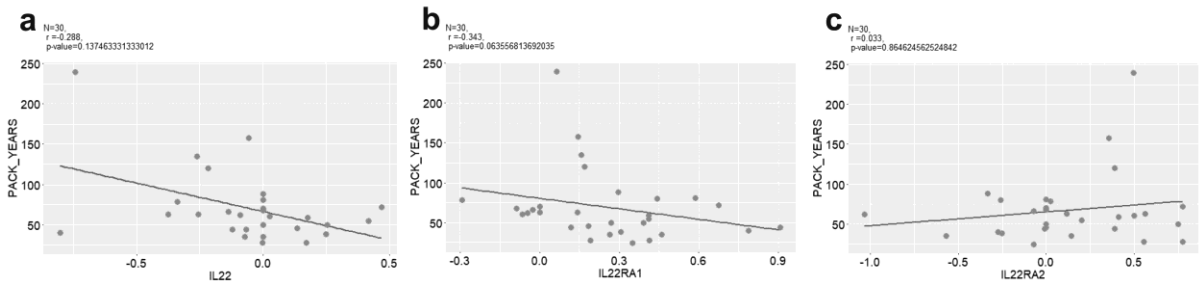
a
N=30
r =-0.288
p-value=0.137463331333012
PACK_YEARS
250
200
150
100
50
-0.5
0.0
0.5
IL22
b
N=30
r =-0.343
p-value=0.063556813692035
PACK_YEARS
250
200
150
100
50
-0.3
0.0
0.3
0.6
0.9
IL22RA1
c
N=30
r =0.033
p-value=0.864624562524842
PACK_YEARS
250
200
150
100
50
-1.0
-0.5
0.0
0.5
IL22RA2

a

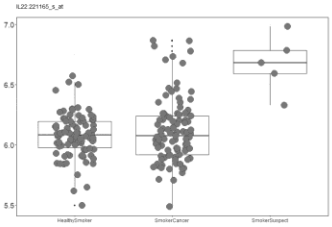
IL22.221165_s_at
7.0
6.5
6.0
5.5
HealthySmoker
SmokerCancer
SmokerSuspect

b

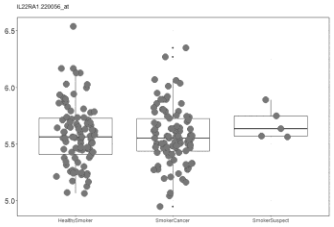
IL22RA1.229056_at
6.5
6.0
5.5
5.0
HealthySmoker
SmokerCancer
SmokerSuspect

c

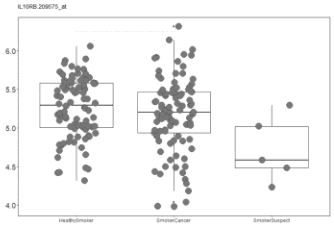
IL10RB.209575_at
6.0
5.5
5.0
4.5
4.0
HealthySmoker
SmokerCancer
SmokerSuspect

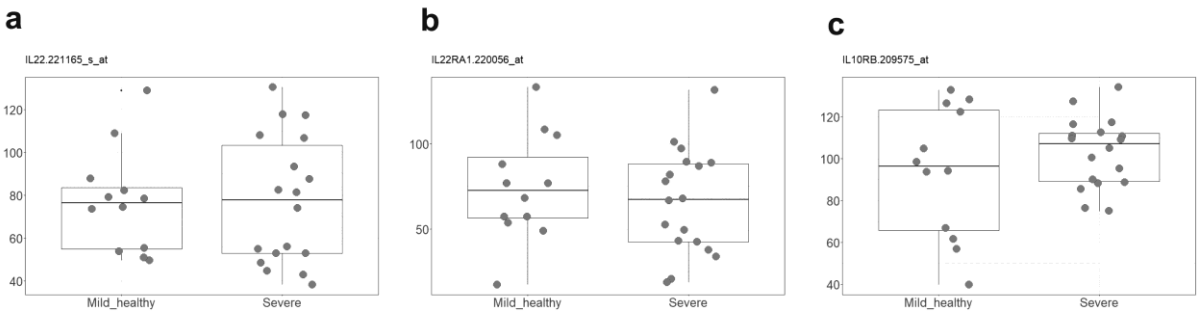
a
IL22.221165_s_at
120
100
80
60
40
Mild_healthy
Severe
b
IL22RA1.220056_at
100
50
Mild_healthy
Severe
c
IL10RB.209575_at
120
100
80
60
40
Mild_healthy
Severe

IL-22

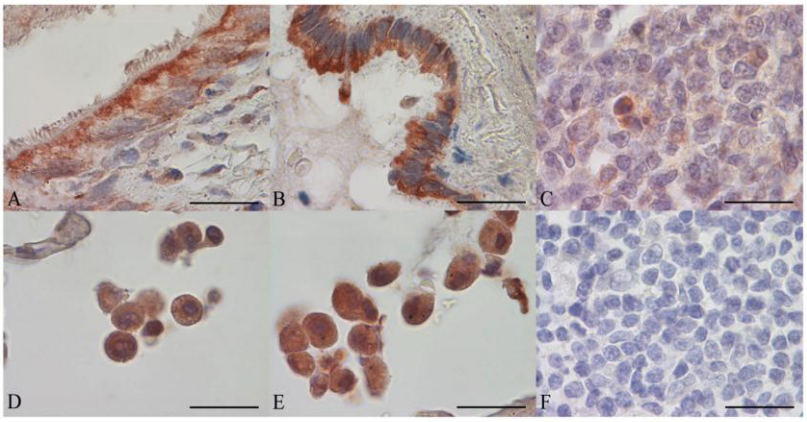

IL-22RA1

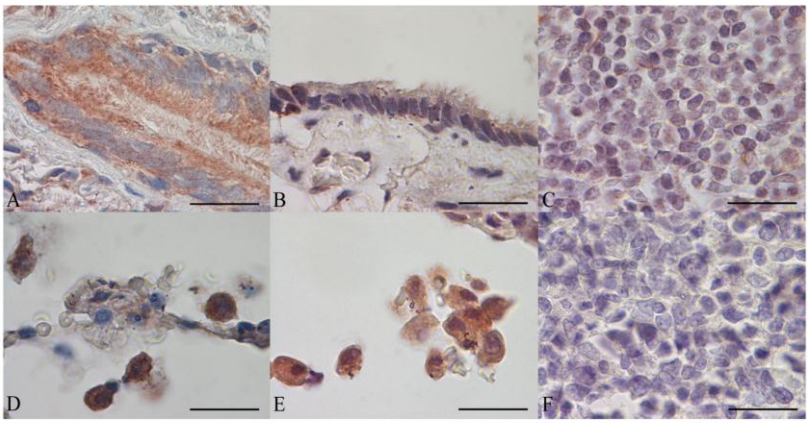

IL-22RA2

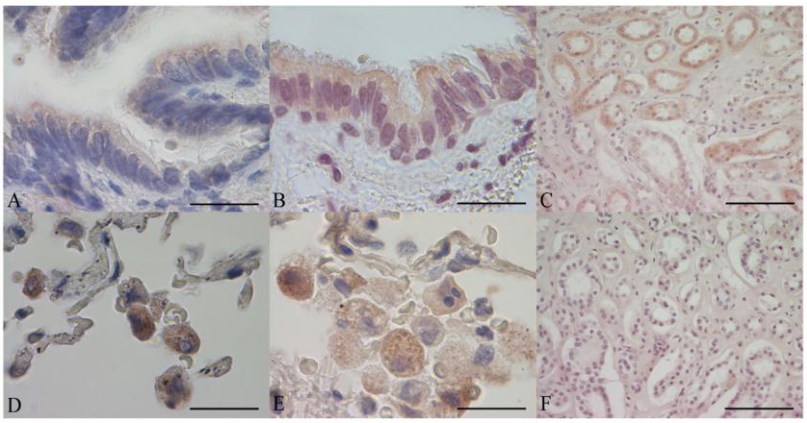

IL-10RB

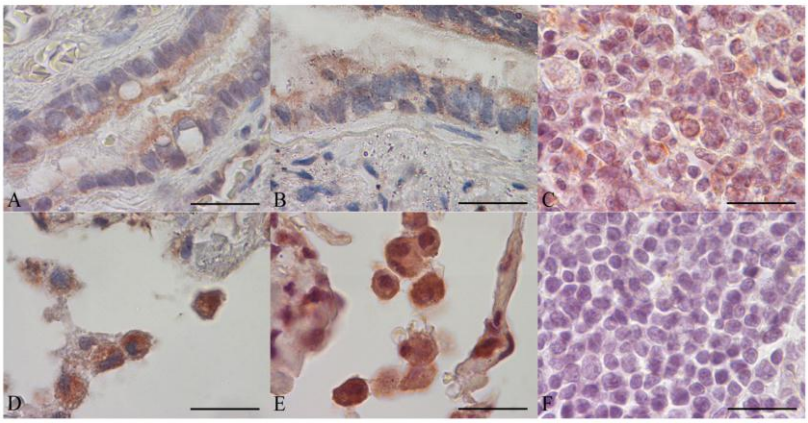

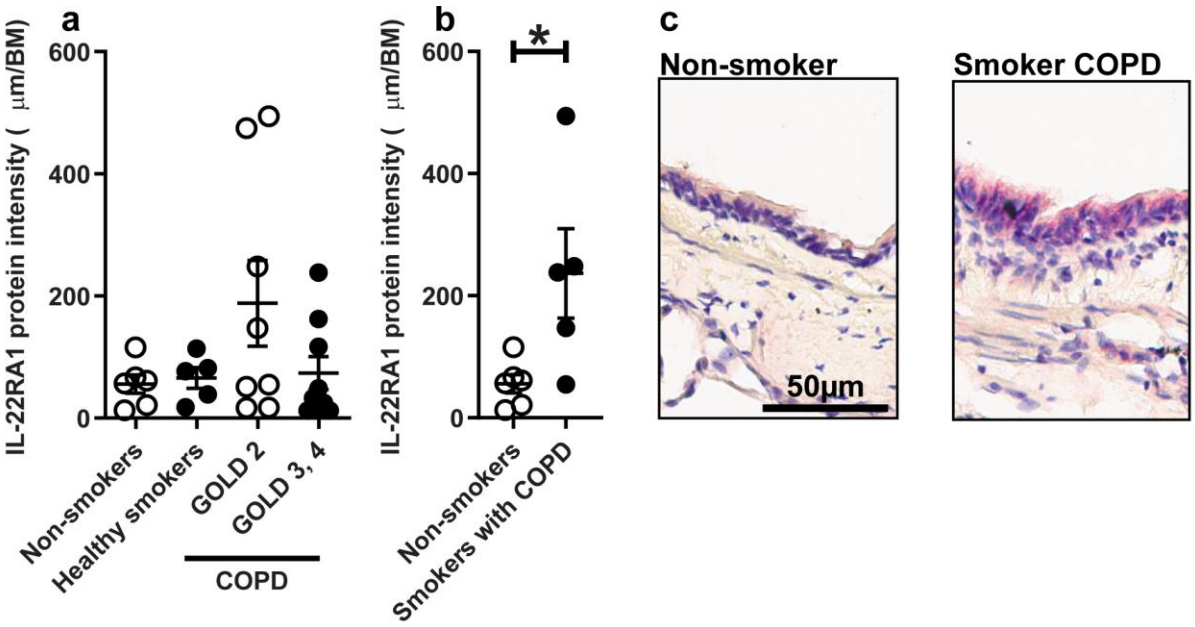
a
IL-22RA1 protein intensity (µm/BM)
600
400
200
0
Non-smokers
Healthy smokers
GOLD 2
GOLD 3, 4
COPD
b
IL-22RA1 protein intensity (µm/BM)
*
600
400
200
0
Non-smokers
Smokers with COPD
c
Non-smoker
50µm
Smoker COPD

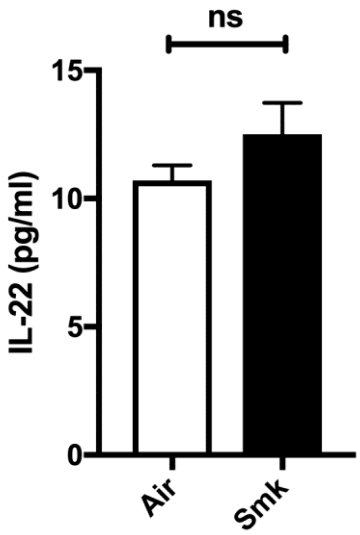
ns
15
10
5
0
IL-22 (pg/ml)
Air
Smk

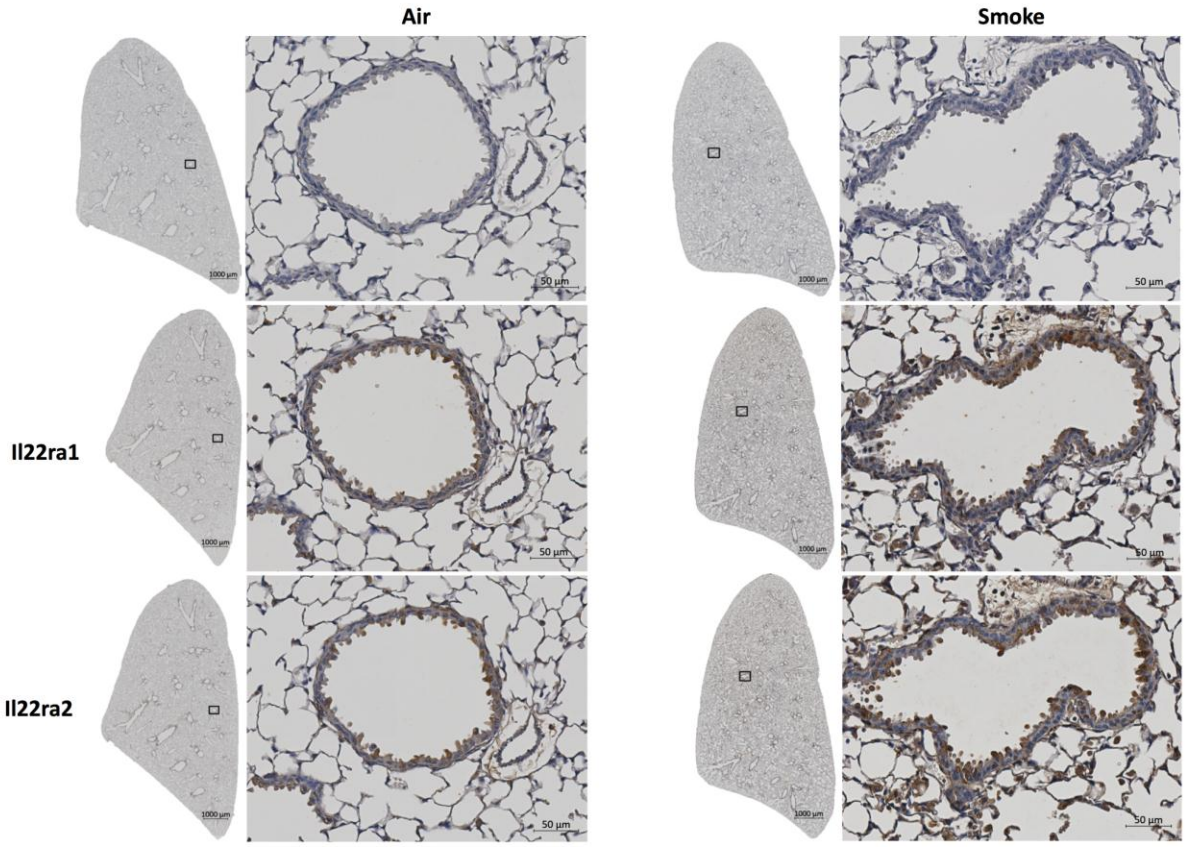
Air
Smoke
Il22ra1
Il22ra2
1000 µm
50 µm

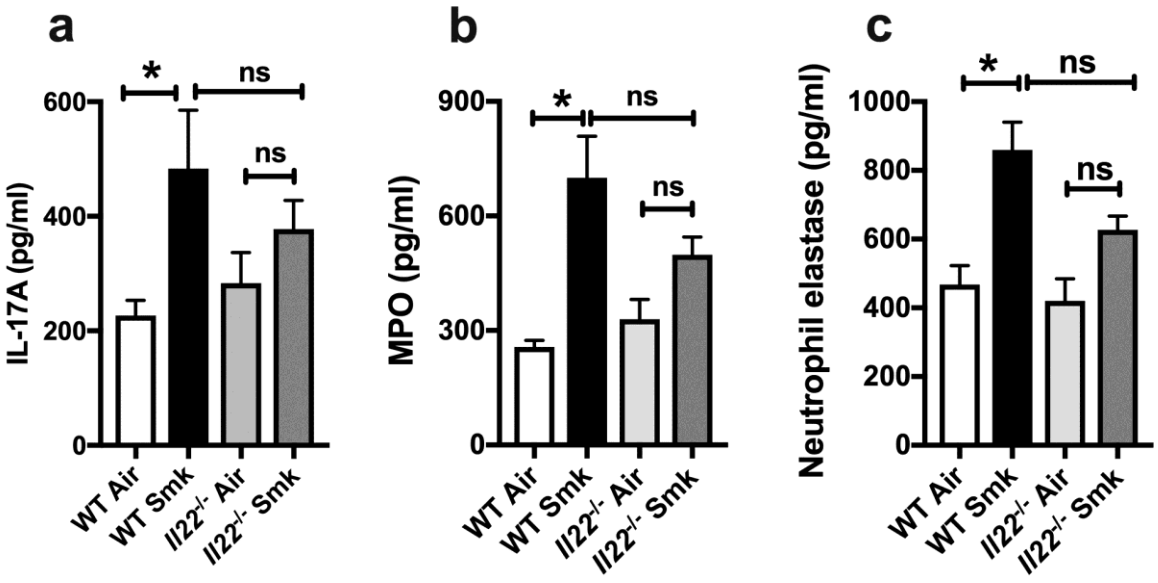
a
b
c
IL-17A (pg/ml)
MPO (pg/ml)
Neutrophil elastase (pg/ml)
0
200
400
600
300
900
800
1000
*
ns
ns
WT Air
WT Smk
Il22-/- Air
Il22-/- Smk

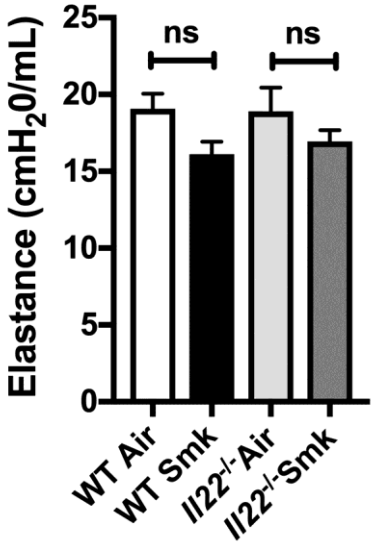
Elastance (cmH20/mL)
25
20
15
10
5
0
ns
ns
WT Air
WT Smk
Il22-/-Air
Il22-/-Smk